1

Synthetic Methods Toward Single-Chain Polymer Nanoparticles

Ozcan Altintas[1], Tobias S. Fischer[2], and Christopher Barner-Kowollik[2,3]

[1] *University of Minnesota, Department of Chemistry, 207 Pleasant St SE, Minneapolis, MN 55455-0431, USA*
[2] *Institut für Technische Chemie und Polymerchemie Karlsruhe Institute of Technology (KIT), Preparative Macromolecular Chemistry, Engesserstraße 18, 76128 Karlsruhe, Germany*
[3] *Queensland University of Technology (QUT), School of Chemistry, Physics and Mechanical Engineering, 2 George Street, QLD 4000, Brisbane, Australia*

1.1 Introduction

Natural macromolecules such as enzymes effectively function due to a precise as well as dynamic three-dimensional (3D) architecture. One of the most important driving forces for synthetic macromolecular design is the emulation of natural processes and the design of chemical reaction sequences that are inspired by nature [1–3]. Nature's degree of controlling the synthesis remains unreached by synthetic chemists. Nevertheless, well-defined compact 3D synthetic functional structures can be prepared, reducing the conformational freedom of single polymer chains by connecting pendant subunits at predefined positions [4–6].

Scientists have been interested in intramolecular cross-linking reactions since the mid-twentieth century where cross-linking processes have been investigated between variable molecules at very low concentrations of polymers in solution [7–9]. Reversible deactivation radical polymerization (RDRP) techniques such as atom transfer radical polymerization (ATRP) [10, 11], reversible addition–fragmentation chain transfer (RAFT) polymerization [12, 13], and nitroxide-mediated polymerization (NMP) [14] are employed to synthesize well-defined polymers by controlling the dispersity, molecular weight, and architecture of the macromolecules. In addition, exploiting the combination of RDRP techniques with modular and orthogonal ligation protocols [15–17], the intramolecular cross-linking of a single polymer chain leading to single-chain nanoparticles (SCNPs), has rapidly emerged as an alternative approach to generate well-defined compact 3D synthetic functional structures with diameters of below 20 nm [18–27]. Supramolecular chemistry affords a high degree of control over naturally occurring molecules and macromolecules [28]. Typically, the formed natural biopolymers and their structure are controlled by reversible self-folding processes induced by supramolecular interactions [29]. Hydrogen bonds, van der Waals interactions, and electrostatic or hydrophobic interactions force biomolecules such as proteins into their 3D folded analog. Folding of

Single-Chain Polymer Nanoparticles: Synthesis, Characterization, Simulations, and Applications,
First Edition. Edited by José A. Pomposo.

proteins, for instance, leads to complex secondary, tertiary, and quaternary structures, which determine their properties and functions [30].

Single-chain folding of synthetic macromolecules has been a fast moving and innovative field in macromolecular chemistry, constituting a promising pathway toward artificial, adaptative, and smart single-chain polymer nanodevices. The folding and unfolding of well-defined single linear polymer chains has been studied by means of single-chain technology [23] through intramolecular bonds from the viewpoint of synthetic macromolecular chemistry [25]. Generally, SCNPs can be generated by two approaches [26]. In one approach, individual – and often mutually orthogonal – recognition motifs are attached to preselected and defined points along the polymer chain, leading to well-defined SCNPs, a process that has been termed "selective-point folding". A second pathway to form SCNPs is the so-called "repeat-unit approach." For repeat-unit folding, block copolymers with specific complementary yet statistically scattered motifs along the polymer backbone are designed. The resulting structures are less defined due to a chaotic and statistical collapse compared with selective-point folding. Single-chain folding technology makes intensive use of supramolecular non-covalent interactions to generate SCNPs. We here focus on the application of irreversible bonds, non-covalent bonds, and dynamic covalent bonds to fold one single polymer chain into a SCNP. The current understanding of how to synthesize well-defined precursor polymers as well as the corresponding SCNPs will be discussed in detail. Our exploration into SCNP synthetic technology commences with a foray into the simplest of all folding systems, that is, rings. Throughout the current chapter, we do not attempt to provide a complete review of the field but will rather focus on critically selected examples.

1.2 Single-Chain Rings via Irreversible and Reversible Bonds

In nature, ring formation is employed to equip polypeptides with specific properties, such as improved stability against enzymatic degradation. In recent years, polymers possessing various topologies have been prepared via advanced modular ligation reactions. Cyclic polymers with an endless molecular topology have gained interest from polymer and material scientists due to their unique physical properties [31, 32]. Cyclic polymers have significantly different characteristics with regard to intrinsic viscosity, glass transition temperature, and order–disorder transition compared with their linear counterparts [33]. A wide variety of cyclization methods has been reported. We submit that the provision of cyclic polymer systems is a key step preceding the preparation of single-chain polymeric nanoparticles. There exist important similarities between the preparation of cyclic polymers and single-chain polymeric nanoparticles in terms of reaction conditions as well as characterization methods. However, the cyclic polymer field is immense, and therefore, we highlight here selected examples only, where the same or similar chemistries were used for the preparation of the SCNPs.

Grayson and coworkers first reported the preparation of single-chain rings based on the combination of ATRP and the copper-catalyzed azide–alkyne

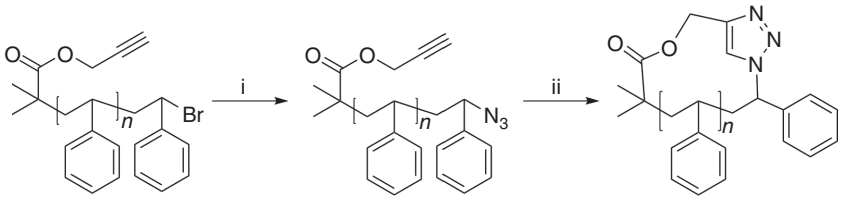

Figure 1.1 Synthetic route for the preparation of well-defined cyclic polystyrene via the combination of ATRP and CuAAC reaction. (i) NaN_3, DMF, room temperature (r.t.). (ii) CuBr/Bipy, in degassed DMF, 120 °C. (Laurent and Grayson 2006 [34]. Reproduced with permission of the American Chemical Society.)

cycloaddition (CuAAC) reaction coupling azide and alkyne-functional end groups (Figure 1.1) [34]. A linear poly(styrene) (PS) precursor was prepared via the ATRP technique, using propargyl 2-bromoisobutyrate as the initiator. Subsequent azidation of the end group was carried out. The cyclization reaction was successfully conducted on α-alkyne- and ω-azide-functionalized linear polymers using a syringe pump system, allowing for very low concentrations (<0.01 mM). The single-chain folding was followed by size-exclusion chromatography (SEC), ^{1}H nuclear magnetic resonance (NMR) spectrometry, and Fourier transform infrared (FT-IR) analysis. The CuAAC reaction has received substantial attention in the field of cyclic polymers [35, 36] due to its often quantitative yields, mild reaction condition, tolerance to a wide range of functional groups, and harmony with the RDRP techniques for the preparation of various cyclic topologies [37, 38].

As an alternative to CuAAC processes, Diels–Alder (DA) cycloadditions involve the reaction of a conjugated diene (4π) with a dieneophile (2π) to yield a 6-membered ring, where the [4 + 2] denotes the number of π-electrons that are taking part in the cycloaddition process. Especially light-triggered DA reactions ensure near quantitative coupling within short reaction times at ambient temperature without a catalyst and are a highly promising avenue for the preparation of cyclic polymers and SCNPs alike. Barner-Kowollik and coworkers introduced a facile method for the preparation of macrocyclic aliphatic polyesters based on the catalyst-free and ambient-temperature intramolecular DA coupling of highly functional photosensitive α-*o*-methylbenzaldehyde and ω-acrylate polyester chains (Figure 1.2) [39, 40]. Polycaprolactone (PCL) and polylactide (PLA) were synthesized via ring-opening polymerization (ROP) using 2-((11-hydroxyundecyl)oxy)-6-methyl-benzaldehyde as an initiator in the presence of triazabicyclodecene (TBD) or 1,8-diazabicyclo[5.4.0]undec-7-ene (DBU) functioning as organocatalysts. The hydroxyl functionality of the linear polymers was reacted with acryloyl chloride to afford a terminal dienophile group. The completion of the end-group transformation was confirmed by ^{1}H NMR and electrospray ionization mass spectrometry (ESI-MS), and the subsequent DA reactions were performed by irradiation of the linear precursor solutions in acetonitrile at ambient temperature at concentrations of 25 mg L^{-1} for 12 h under ultraviolet (UV) light ($\lambda_{max} = 320$ nm). The cyclic products were collected by evaporation of the solvent without the need for additional purification steps and confirmed by SEC, ^{1}H NMR, and ESI-MS. In the same context, Zhang and coworkers developed a method for the formation

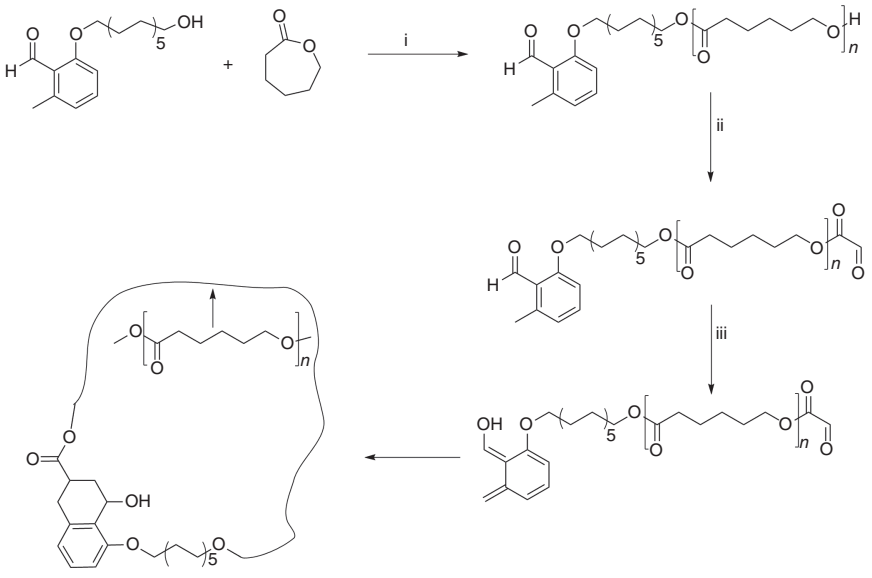

Figure 1.2 Synthetic route for the preparation of cyclic poly(ε-caprolactone). (i) 1,5,7 Triazabicyclo[4.4.0]dec-5-ene (TBD), CH_2Cl_2, r.t. (ii) Acryloyl chloride, triethylamine, tetrahydrofuran (THF), r.t. (iii) hν (λ_{max} = 320 nm), acetonitrile, r.t. (Josse *et al*. 2013 [39]. Reproduced with permission of the Royal Society of Chemistry.)

of various types of cyclic homopolymers and block polymers by a combination of RAFT polymerization and a light-induced DA click reaction [41], based on synthetic technology we introduced (light-induced hetero-DA chemistry) [42]. In following work by the same research group, an efficient and practical way was investigated to produce cyclic polystyrenes on a large scale by the combination of continuous flow techniques and UV-induced DA reactions [43]. In an alternative light-triggered approach, Yamamoto and colleagues [44] successfully demonstrated the intramolecular dimerization reactions of the anthryl and coumarinyl end-group-functionalized polymers both in water and organic solvents.

Thiol–ene reactions have recently been used for a variety of synthetic processes including single-chain ring formation [45, 46]. For example, Zhang and coworkers reported a straightforward approach for the one-pot synthesis of cyclic polymers via thiol-Michael addition [47]. Linear precursor polymers were prepared via RAFT polymerization using a chain transfer agent (CTA) with furan-protected maleimides at the R group. A highly diluted solution (0.014 mM) of polymethyl methacrylate (PMMA) was prepared, and subsequently the maleimide was deprotected at 110 °C followed by aminolyzing the thiocarbonylthio to a thiol group at ambient temperature. Upon the release of the thiol, the cyclic PMMA was obtained through intramolecular ring closure via thiol–maleimide Michael addition. The cyclic PMMA was subjected to SEC, NMR, and matrix assisted laser desorption ionization-time of flight (MALDI-TOF) MS, which provided convincing evidence for the successful preparation of the cyclic structures.

In related work, Monteiro and coworkers demonstrated a versatile strategy for the cyclization of RAFT-based polymers in a one-pot synthesis using the thiol–ene or thio–bromo reaction [45]. The heterodifunctional trithiocarbonate RAFT agent featuring an alkyne functionality was designed to mediate the RAFT polymerization of various monomers, and subsequently either activated acrylate or bromine functionalities were installed at the chain end of the polymer via an esterification reaction. Hexylamine was used to convert the RAFT end group to a free thiol moiety, which reacted with the acrylate on the other chain terminus to afford the cyclic polymer. The overall results indicate that the thiol–ene cyclization reaction was more successful than the thio–bromo reaction.

Reversible self-folding processes are nature's way to control the conformation of biological polymers, and specifically the disulfide bridges employed within by natural proteins provide a robust system for dynamic single-chain systems adaptable by external stimuli. In an interesting approach, Du Prez and coworkers developed an efficient synthetic pathway toward cyclic polymers based on the combination of thiolactone and disulfide chemistry (Figure 1.3) [48]. An α-thiolactone and an ω-dithiobenzoate functional linear polystyrene was prepared via RAFT polymerization using a newly designed CTA and subsequent conversion of the dithioester end groups to thiols through aminolysis. The single cyclic PS-featuring disulfide linkage was constructed under highly diluted conditions, allowing for the one-step preparation of functionalized cyclic

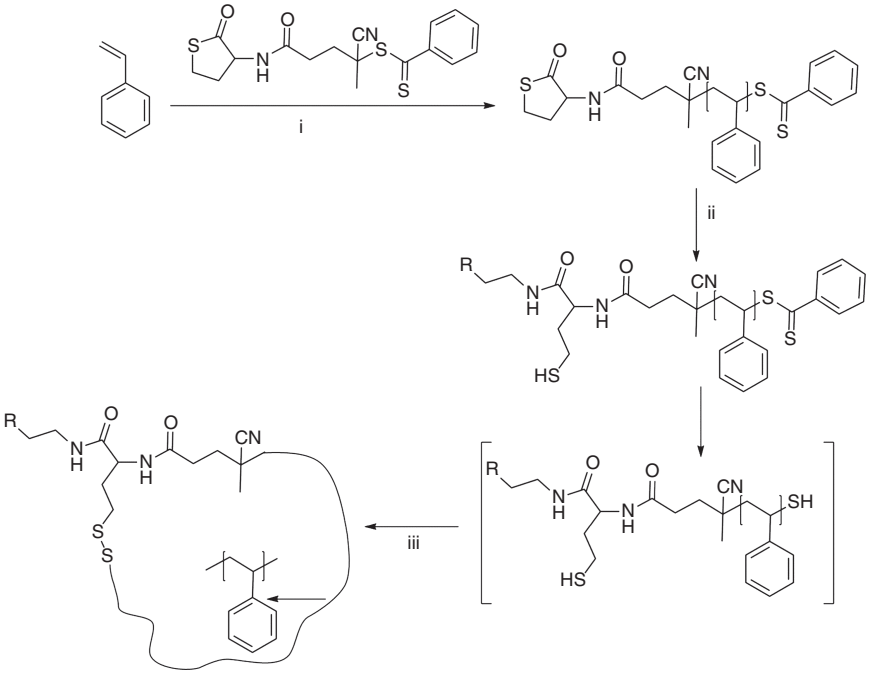

Figure 1.3 Combined RAFT and thiolactone approach toward functionalized cyclic polymers. (i) RAFT polymerization. (ii) Propylamine or ethanolamine, dichloromethane (DCM). (iii) DCM, 2 days. (Stamenović *et al*. 2012 [48]. Reproduced with permission of the Royal Society of Chemistry.)

polymers with high yields. The cyclic PS disulfide ring formation was evidenced by SEC, MALDI-TOF MS, and ^{1}H NMR characterization. Furthermore, the topological transformation (folding/unfolding) was demonstrated by either disulfide reduction or thiol–disulfide exchange reactions.

Many proteins undergo folding in solution to yield delicate molecular assemblies stabilized by non-covalent interactions such as hydrogen bonds. Barner-Kowollik and coworkers reported the first examples for single-chain folding of α,ω-complementary hydrogen bonding motif functional polymer strands prepared by a combination of ATRP and the CuAAC reaction in the context of macromolecular mimicry of naturally occurring proteins (Figure 1.4) [49]. While a cyanuric acid (CA) functional ATRP initiator provides for the α-end of the macromolecules, the Hamilton wedge (HW) was inserted into the ω-end of the polymer strands via CuAAC. Single-chain self-folding of the macromolecules at concentrations of below <1 mM was supported by ^{1}H NMR and dynamic light scattering (DLS) analyses. A further related example was presented by our team utilizing thymine (Thy) and diaminopyridine (DAP) as the hydrogen bonding complementary motifs [50]. A well-defined heterotelechelic polystyrene was prepared by ATRP as well as CuAAC, where the Thy and the DAP recognition units were attached to the macromolecules in the α,ω-position, respectively, and subsequently single-chain folding of the polymer was studied in detail using the same methods as in the previous publication. In related work by Barner-Kowollik and coworkers, the preparation of a well-defined triblock homopolymer featuring two pairs of mutually orthogonal hydrogen bonding motifs (CA–HW and thy–DAP) at well-defined points within the polymer chain was first described [51]. Initially, the orthogonality of the motifs (CA, HW, Thy, DAP) was confirmed by ^{1}H NMR spectroscopy between small molecules. In our study, the CA functionality was located at the α-position of the polystyrene chain by virtue of a functional ATRP initiator, while the Thy and the DAP functionalities were inserted at preselected positions on the polymer backbone. The HW functionality was attached at the ω-position of the linear polymer chain with a combination of ATRP and the CuAAC reaction. The single-chain folding/unfolding processes of the linear triblock homopolymers were followed by ^{1}H NMR spectroscopy in tetrachloroethane at variable temperatures and low concentrations, evidencing the hydrogen bonding interactions between the Thy–DAP and CA–HW units. DLS as well as static light scattering (SLS) analyses of the macromolecular self-assembly systems in diluted solution further evidenced the formation of single-chain self-folded structures.

In another example, Barner-Kowollik and coworkers reported the preparation of well-defined 8-shaped cyclic diblock copolymers via single-chain hydrogen bonding-driven selective-point folding [52]. The well-defined linear polystyrene and poly(*n*-butyl acrylate) carrying complementary recognition units were synthesized via activators regenerated by electron transfer (ARGET) ATRP utilizing functional initiators. The orthogonal hydrogen bonding recognition motifs were incorporated into the polymer chain ends of the respective building blocks. Diblock copolymer formation was successfully carried out via a CuAAC reaction. The concentration regime <10 mg mL^{-1} for the single-chain formation was

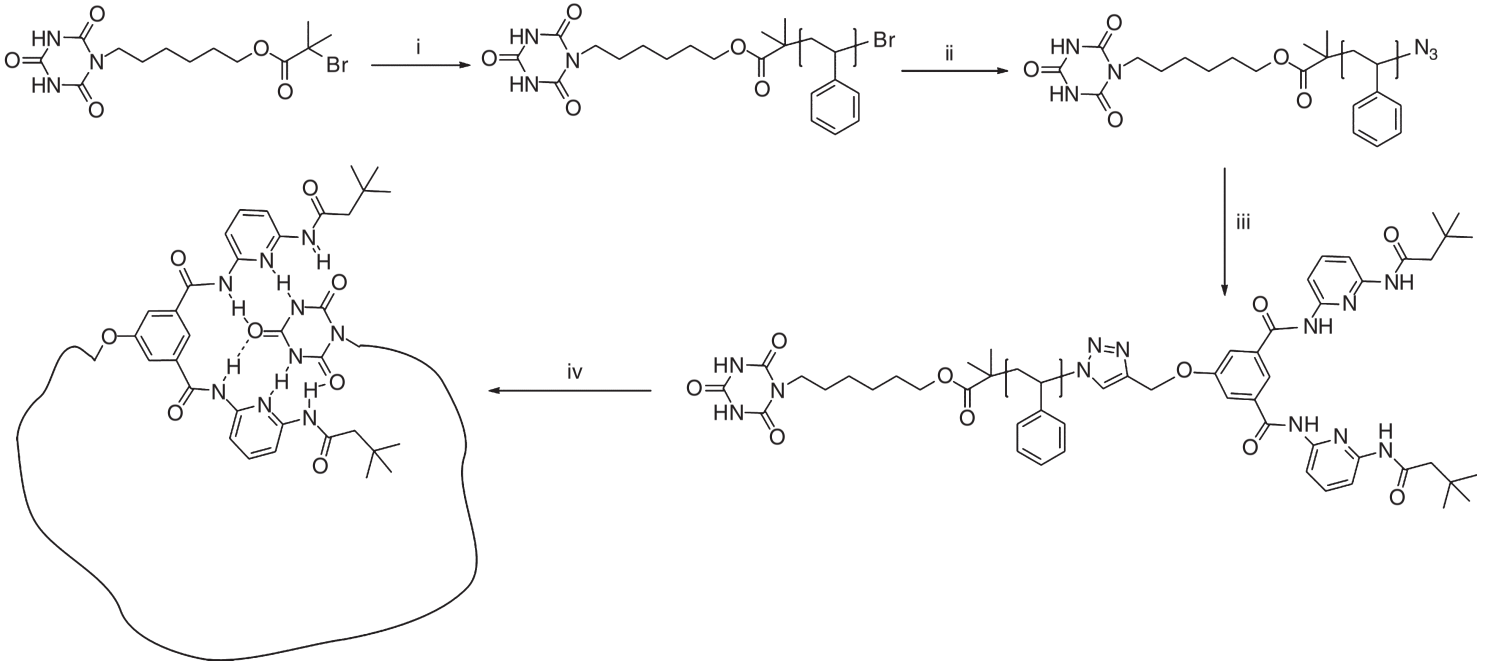

Figure 1.4 General strategy for preparing α,ω hydrogen donor/acceptor functional polymers and their subsequent single-chain self-assembly. (i) CuBr, PMDETA, styrene, anisole, 90 °C. (ii) NaN_3, DMF, r.t. (iii) $CuSO_4 \times 5\ H_2O$, sodium ascorbate, DMF, alkyne functional HW. (iv) High dilution in DCM. (Altintas *et al.* 2010 [49]. Reproduced with permission of the Royal Society of Chemistry.)

determined by diffusion-ordered spectroscopy (DOSY) NMR at ambient temperature indicating the concentration limit for single-chain folding.

A second and versatile class of supramolecular motifs that are used for single-chain folding are host–guest systems. Harada and coworkers were the first to perform the reversible folding of a polymer in aqueous conditions with the CD-azobenzene (AB) host–guest motif [53]. We investigated the reversible folding behavior of well-defined polymers carrying the CD and adamantyl (AD) motif at the chain ends in aqueous media [54]. An α-CD, ω-AD-functionalized poly(*N*,*N*-dimethyl acrylamide) (PDMAa) was initially synthesized by a combination of RAFT polymerization and CuAAC reactions with a novel bifunctional RAFT agent. The single-chain folding through the CD–AD host–guest complexation occurs at concentrations lower than 0.6 mM, whereas higher concentrations led to chain opening and intermolecular aggregation.

Barner-Kowollik and coworkers published the first study on the selective-point folding of a single polymer chain induced by metal–ligand complexation using palladium and triphenylphosphine as a ligand [55]. Dibromo functional polystyrene was synthesized via ARGET ATRP, and subsequently the chain ends of the linear polymer were functionalized with alkyne triphenylphosphines to obtain polymeric macroligands. The addition of palladium (II) ions via a syringe pump leads to the controlled folding of the polymer chain. ^{31}P NMR spectroscopy revealed the success of the Pd complexation, which results in a significant shift of the macroligand resonance from −4.99 to 23.53 ppm. Additionally, the single-chain ring formation was characterized by DLS and SEC.

The preparation of cyclic polymers can be considered the simplest form of SCNP preparation, and thus the two fields are strongly intertwined. Herein, selected examples of single-chain ring formation have been highlighted. Importantly, the highlighted modular ligation reactions, which have been used for the preparation of cyclic polymers, can be readily adopted as an orthogonal approach for the preparation of true SCNPs.

1.3 Single-Chain Nanoparticles via Irreversible Bonds

Several modular ligation chemistries have been applied to generate SCNPs from linear precursors possessing cross-linkable functionalities. The following reactions have been extensively employed as cross-linking processes to construct SCNPs, that is, dimerization of benzocyclobutene (BCB), CuAAC, Glaser–Hay coupling, thiol–ene/thiol–yne chemistry, modification of reactive groups by reaction with amines/alcohols/thiols, thiol–disulfide exchange, DA reactions, Michael-type addition, modification of ketones and aldehydes with amines/alkoxyamines/hydrazines, and intramolecular polymerizations. In the following section, the preparation of SCNPs by modular ligation reactions is explored in detail as only few of these reactions have been introduced in the previous section.

The initial examples of intramolecular cross-linking of macromolecules were studied in the 1950s in very diluted solutions where terephthalaldehyde

was added to an aqueous solution of polyvinyl alcohol. Intermolecular and intramolecular reactions were investigated by following the viscosity of the solution. Intramolecular cross-linking reactions were observed in diluted solutions, whereas the intermolecular cross-linking predominated in concentrated systems [7–9, 56]. However, herein we focus on recent examples of intramolecular cross-linking reactions based on functional precursor polymers prepared via advanced polymerization methods. In early studies in the field, the BCB moiety was intensively used for the preparation of SCNPs. Several approaches for the controlled intramolecular folding of linear polymer chains to afford well-defined single-molecule nanoparticles were developed by Hawker and colleagues (refer to Figure 1.5) using BCB motifs as intramolecular cross-linking agents forming benzoquinone dimethanes [57–59]. In early studies, linear precursor polymers containing numerous latent coupling groups along the backbone were prepared by copolymerization of styrene and BCB functional monomer. A solution of the BCB-functionalized linear polymer was added to a benzyl ether solution without any intermolecular cross-linking reaction by continuous addition of the precursor polymer solution to hot benzyl ether at 250 °C, thus achieving a low concentration of the linear precursor in the solution. The resulting SCNPs were readily characterized by standard techniques such as SEC, DLS, ^{1}H NMR spectroscopy, and differential scanning calorimetry (DSC). For example, the starting linear polymer features a number average molecular weight, M_n, of 84.8 kDa; however, upon intramolecular reaction, the hydrodynamic volume of the macromolecule decreases to an apparent M_n of 59 kDa to yield the SCNP. Subsequently, Harth and coworkers suggested alternative benzoquinone dimethane cross-linking precursors for intramolecular chain collapse nanoparticles inspired by BCB chemistry employing a novel vinylbenzosulfone (VBS) cross-linking unit for the preparation of well-defined nanoparticles [60]. The cross-linking unit was synthesized by a five-step pathway, which requires only two purification steps. Random copolymers of styrene and the VBS unit were synthesized via the NMP method with excellent control over molecular weight and with low polydispersity in the presence of R-hydrido alkoxyamine. After successful incorporation of the novel *o*-chinodimethane precursor into the polystyrene, the intramolecular chain collapse process was carried out in

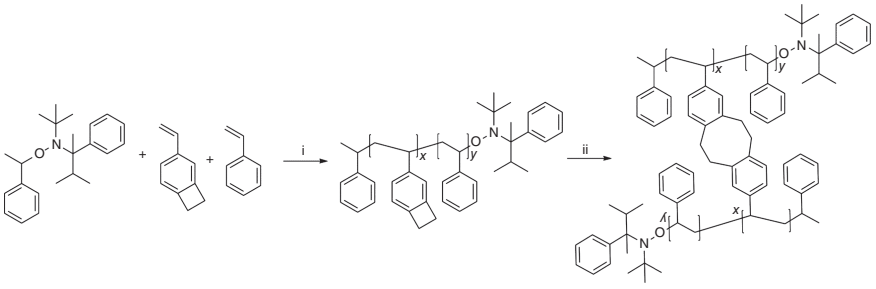

Figure 1.5 Synthesis of benzocyclobutene-functionalized linear polystyrene and schematic representation of the intramolecular collapse of the linear polymer. (i) 120 °C. (ii) 250 °C. (Harth *et al*. 2002 [57]. Reproduced with permission of the American Chemical Society.)

dibenzyl ether to form *o*-quinodimethane intermediates, leading to well-defined monodisperse nanoparticles of 5–10 nm size dimensions at temperatures close to 250 °C. SCNPs formation was applied to the field of conducting copolymers, for example, the synthesis of polymeric nanoparticles from single ABA-type block copolymers in an intramolecular chain process was presented by Harth and coworkers [61]. ABA triblock copolymers were prepared from conducting polymers such as fluorene homopolymers and fluorene/thiophene copolymers designed as telechelic macroinitiators to facilitate NMP methods. The polymerization with styrene and VBS cross-linking units led to the desired ABA triblock copolymers with various ratios of the polymer copolymer blocks. In an intramolecular chain collapse process, the ABA triblock copolymers formed well-defined SCNPs with the confined semiconducting polymer block B as core unit via a controlled cross-linking of the benzosulfone unit within the A block copolymer. Photoluminescence measurements illustrate the influence of the molecular weight of the A block to be crucial for the site isolation of the embedded conducting polymer block in the resulting nanoparticles with quantum efficiencies of 6%. The quantum efficiency of the formed polymeric nanoparticles (6%) was three times higher in comparison to the linear precursor (2%). Most recently, a new synthetic pathway was presented by Hart and coworkers for the preparation of polyacrylate nanoparticles through an intramolecular chain collapse reaction at relatively low temperatures [62]. Poly(acrylic acid) was synthesized by RAFT, and subsequently an amine functional BCB was grafted to the polymer through chloroformate activation chemistry. The BCB-based cross-linking unit permits the reduction of the temperature to close to 100 °C for the formation of the polymeric nanoparticles.

Due of their often quantitative conversions, mild reaction condition as well as tolerance to several functional units, copper-catalyzed reactions are often employed within the field of SCNPs [63–65]. For example, Loinaz and coworkers described a new synthetic route and highly efficient ambient temperature synthetic method based on single-chain intramolecular CuAAC reactions [66]. Introduction of coupling precursors into the PMMA chains was simply performed by polymerization of methyl methacrylate (MMA) in the presence of small stoichiometric amounts of azide- and protected alkyne-containing methacrylate comonomers at three concentrations (4, 7, and 10 mol%) using the RAFT polymerization technique. One-pot deprotection of the propargyl monomer units in the terpolymer was performed followed by a single-chain intramolecular CuAAC reaction at ambient temperature using a CuI salt and a continuous addition technique. The CuAAC reaction induces an intramolecular collapse of the linear chains to individual polymeric nanoparticles resulting in a significant reduction of the hydrodynamic volume and no significant change in polydispersity as observed by SEC. In addition, the terpolymers containing an excess of azide moieties (over-stoichiometric protected alkyne moieties) were prepared by RAFT polymerization, and subsequently the polymeric nanoparticles with an excess of azide groups reacted with propargyl glycine. This versatile and general method opens a way for the synthesis of other kinds of polymeric and bioconjugated nanoparticles. Furthermore, SCNPs were prepared

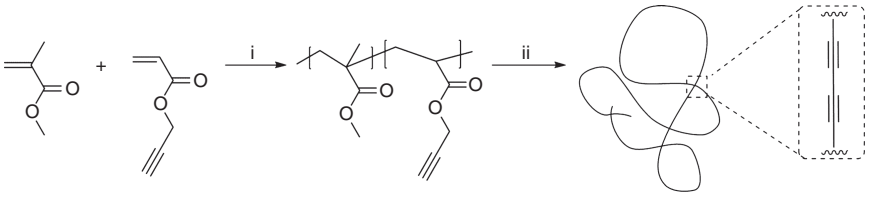

Figure 1.6 Single-chain nanoparticle construction at 25 °C under normal air atmosphere from naked P(MMA-*co*-PgA) precursor copolymers via the Glaser–Hay alkyne coupling reaction. (i) CPDB, BPO/NNDMANIL, THF, 25 °C. (ii) CuI, TMEDA, Et_3N, THF, air, 25 °C. (Sanchez-Sanchez *et al*. 2012 [67]. Reproduced with permission of John Wiley and Sons.)

by Pomposo and coworkers using the copper-catalyzed Glaser–Hay alkyne coupling reaction as well as redox-initiated RAFT polymerization (Figure 1.6) [67]. Redox-initiated RAFT polymerization of MMA and propargyl acrylate (PgA) at ambient temperature by the benzoyl peroxide (BPO)/*N*,*N*-dimethylaniline (NNDMANIL) redox pair using 2-cyanoprop-2-yl-dithiobenzoate (CPDB) as chain transfer agent allows for the synthesis of a variety of precursor polymers ($Đ = 1.12–1.37$ up to $M_w = 100$ kDa). Importantly, linear precursor polymers containing unprotected acetylenic functional groups were readily prepared by redox-initiated RAFT polymerization. After careful screening of the reaction conditions based on copper-catalyzed carbon–carbon coupling (Glaser–Hay coupling) of low-molecular-weight model compounds, nanoparticle synthesis was performed in THF under air atmosphere at 25 °C in the presence of Et_3N, using catalytic amounts of CuI and *N*,*N*,*N*,*N*-tetramethylethylenediamine (TMEDA).

Thiol–ene or thiol–yne radical addition reactions can be carried out under UV irradiation in the presence of a photoinitiator (without using transition metal catalysts) between a thiol and an alkene or an alkyne, resulting in thioether products with a high degree of anti-Markovnikov selectivity [68]. For example, Pomposo and colleagues reported a strategy for the rapid, efficient synthesis of SCNPs (Figure 1.7) [69]. Precursors were prepared via ambient-temperature redox-initiated RAFT polymerization in THF of MMA and allyl methacrylate (AMA) or PgA in the presence of CPBD as CTA and a nearly equimolar ratio of NNDMANIL/BPO as redox initiator system. The SCNPs were prepared from the precursor polymers by photoactivated radical-mediated thiol–ene coupling (TEC) and thiol–yne coupling (TYC) using 3,6-dioxa-1,8-octane-dithiol (DODT) as homobifunctional cross-linker and 2,2-dimethoxy-2-phenylacetophenone (DMPA) as photoinitiator. The reactions were carried out in THF in high dilution at ambient temperature for 90 min. Confirmation of SCNP formation was carried out by means of SEC/multi-angle light scattering (MALLS), ^1H NMR, and transmission electron microscopy (TEM) measurements. SCNPs can be prepared at concentrations ≤ 0.5 mg mL^{-1} based on the SEC/MALLS analysis.

UV light-induced cycloadditions often constitute an alternative, convenient, atom-efficient reaction class for single-chain folding that can be carried out quantitatively at ambient temperature without the need for any metal catalyst. A number of photo-induced reactions have been examined for SCNP

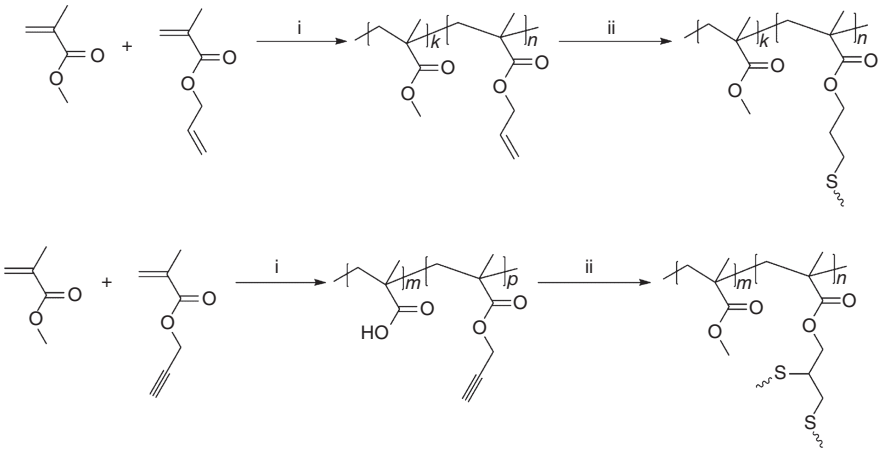

Figure 1.7 Synthetic strategy for the preparation of SCNPs through photoactivated thiol–ene and thiol–yne reactions. (i) THF, BPO/NNDMANIL, CPBD, r.t., 17 h. (ii) 3,6-dioxa-1,8-octane-dithiol, DMPA, THF, UV light irradiation at 300–400 nm, r.t., 90 min. (Perez-Baena *et al*. 2014 [69]. Reproduced with permission of the American Chemical Society.)

formation including light-induced DA reactions [70], photo-induced Bergman cyclizations [71], photo-induced nitrile–imine-mediated tetrazole–ene cycloadditions [72, 73], photo-cross-linking of azide functional polymers [74], and photo-dimerizations of anthracene [75], coumarin [76, 77], and cinnamoyl [78, 79]. For example, Hu and coworkers demonstrated the fusion of photo-Bergman cyclization and intramolecular chain collapse toward polymeric nanoparticles. Employing enediynes as cross-linking precursors, namely, photo-triggered Bergman cyclization, was integrated with an intramolecular chain collapse to generate polymeric nanoparticles within the size regime below 20 nm. The enediyne motif was designed judiciously to possess a high photoreactivity, with the double bond locked in a methyl benzoate ring with the triple bonds substituted with phenyl moieties. Single-electron transfer living radical polymerization (SET-LRP) was conducted to provide linear acrylate copolymers with controlled molecular weights and narrow polydispersities. The polymer bearing an enediyne cross-linker underwent a UV-induced Bergman cyclization, resulting in well-defined polymeric nanoparticles. A series of other acrylate-based nanoparticles were investigated to confirm the applicability of such a unique strategy for thermally sensitive species, but UV-stable polymeric structures, making photo-Bergman cyclization a promising tool toward polymeric nanoparticles. In a study exploiting a unique photochemically induced cycloaddition, Barner-Kowollik and coworkers introduced a new ambient-temperature synthetic approach for the preparation of the SCNPs under mild conditions using a UV light-triggered DA reaction for the intramolecular cross-linking of single polymer chains (Figure 1.8) [70]. Well-defined random copolymers with varying contents of styrene (S) and 4-chloromethylstyrene (CMS) were synthesized employing an NMP initiator, functionalized with a terminal alkyne moiety. Post-modification of the polymers with 4-hydroxy-2,5-dimethylbenzophenone

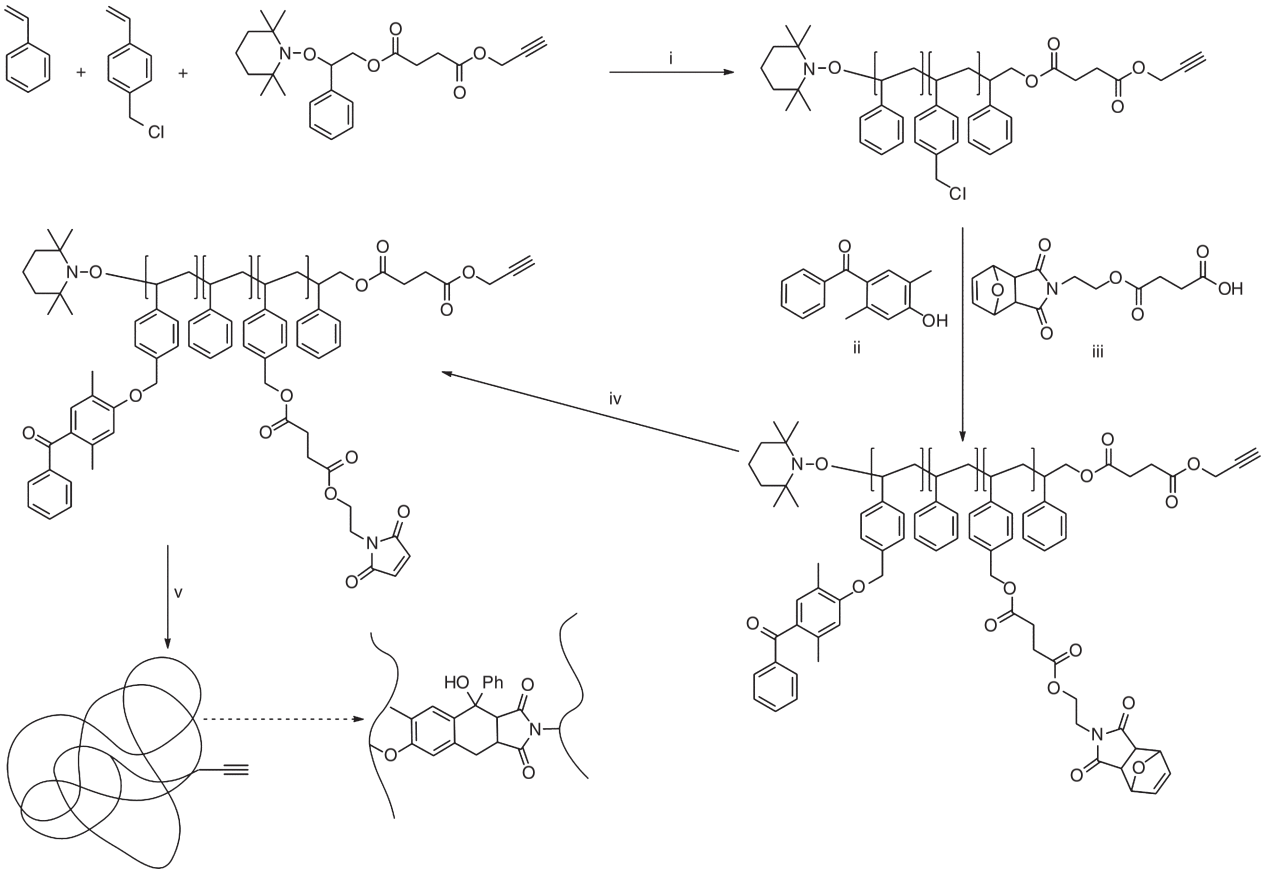

Figure 1.8 Synthetic strategy for the preparation of monofunctional single-chain polymeric nanoparticles. (i) 125 °C, 6 h. (ii) DMF, K_2CO_3, 70 °C, 15 h. (iii) DMF, K_2CO_3, r.t., 24 h. (iv) Toluene, 100 °C, 15 h. (v) DCM, hν (λ_{max} = 320 nm), 30 min. (Altintas *et al*. 2013 [70]. Reproduced with permission of the Royal Society of Chemistry.)

(DMBP) and an *N*-maleimide (Mal) derivative led to the functional linear precursor copolymers in a one-pot/two-step fashion. The intramolecular cross-linking was performed by activating the DMBP groups via irradiation with UV light of 320 nm for 30 min in diluted solution ($c_{\text{Polymer}} = 0.017\ \text{mg mL}^{-1}$). The ensuing DA reaction between the activated DMBP and the Mal groups resulted in well-defined single-chain polymeric nanoparticles. To control the size of the SCNPs, random copolymers with varying CMS contents with various functional group densities (FGDs) were employed for the single-chain collapse. In addition, monotethered nanoparticles were prepared via a CuAAC reaction between the alkyne-bearing copolymer with the highest FGD and an azide-terminated PEG prior to UV-induced cross-linking. The formation of SCNPs was followed by SEC, NMR spectroscopy, DLS, and atomic-force microscopy (AFM). Photochemical processes can also lead to SCNPs with specific property profiles. In an alternative light-triggered approach, Barner-Kowollik and coworkers introduced the facile ambient-temperature generation of size tunable and well-defined fluorescent SCNPs [72]. Importantly, this modular ligation reaction can be performed under mild reaction conditions with quantitative conversion and no by-products except nitrogen. Here, precursor copolymers were synthesized by NMP of styrene and 4-(chloromethyl)-styrene with 2,2,6,6-tetramethyl-1-(1-phenylethoxy)piperidine as the initiator at 125 °C. The lateral chlorine atoms were substituted by protected maleimides as well as tetrazole species in various ratios. The intramolecular cross-linking of the linear precursors was carried out under UV irradiation in highly diluted solutions ($c_{\text{precursor}} = 0.017\ \text{mg mL}^{-1}$) to afford SCNPs, characterized by SEC, DLS, UV/Vis-, and fluorescence spectroscopy. While the above photochemical collapse was based on nitrile–imine intermediates, Berda and coworkers introduced intrachain photodimerization of pendant anthracene units as an efficient route to SCNP fabrication [75]. 9-anthracenylmethyl methacrylate (AMMA) was synthesized in one step from commercially available reagents. Copolymers of MMA with varying amounts of AMMA incorporation were prepared by RAFT polymerization. The formation of polymeric nanoparticles was carried out via intramolecular photodimerization of pendant anthracene units by irradiating dilute solutions of the copolymer in THF with 350 nm centered UV light, confirmed via UV–vis spectroscopy. In addition, irradiation with 254 nm centered UV light results in the partial cleavage of the anthracene photodimers imparting a dynamic character to the SCNPs.

Interestingly, polymerization methods themselves constitute an alternative avenue for the preparation of SCNPs through intramolecular polymerization such as free radical polymerization [80, 81], oxidative polymerization [82], olefin metathesis of allyl groups [83, 84], polycondensation of silane moieties [85], carbazole units [86], and ROP of lactones [87, 88]. For example, synthesis and characterization of amine-functionalized polystyrene nanoparticles were presented by Thayumanavan and colleagues [81]. The primary polymer structures were synthesized by RAFT polymerization using boc-protected 4-vinylaniline and CMS as the chloromethyl styrene monomer, affording the handle for incorporating the needed functionality to induce intramolecular cross-linking, while the protected amino group provides the necessary functionality display in

the final polymeric nanoparticle. The chloromethyl functionality of the copolymers were reacted with 4-[(3-hydroxyphenoxy)-methyl]styrene to afford the corresponding vinyl-functionalized cross-linkable polymers. This cross-linking reaction was carried out under free radical polymerization conditions using AIBN as the initiator in refluxing THF under dilute conditions. The cross-linked polymers were characterized by SEC, NMR, DLS, and AFM, confirming the intramolecular cross-linking process. There are significant differences between the linear polymers and polymeric nanoparticles in AFM analysis, as the precursor polymers exhibit a wormlike structure, while narrowly dispersed nanoparticles were obtained through the cross-linking reaction. In the same context, Coates and coworkers presented a new method for the formation of polymeric nanoparticles by intramolecular cross-linking [89]. The synthesis of polycarbonates with vinyl functionality was achieved through the terpolymerization of cyclohexene oxide (CHO), vinylcyclohexene oxide (VCHO), and CO_2 with a β-diiminate zinc(II) acetate catalyst. Aliphatic polycarbonates with pendant vinyl groups were transformed into nanoparticles through intramolecular olefin cross-metathesis. Importantly, at high concentrations of precursor polymer (>10 mg mL^{-1}), intra- and intermolecular cross-linking reactions occurred, indicating an increase in M_n and a broadening of $Đ$ based on SEC, whereas the apparent molecular weight decreased and the molecular weight distribution remained narrow in dilute polymer solutions (1 mg mL^{-1}), suggesting that only intramolecular cross-linking occurred. The formation of macromolecular nanoparticles was also confirmed by AFM showing the unreacted polymer reveals extended molecules; however, the majority of the cross-linked molecules were visualized as isolated particles, providing further support, along with SEC, for intramolecular cross-linking under dilute conditions. In an interesting recent study achieving SCNPs in relatively high concentration (close to 100 mg mL^{-1}), Qiao and coworkers reported the formation of single-chain polymeric nanoparticles prepared via ROP (Figure 1.9) [87]. Various linear random copolymers, poly(oligo(ethylene glycol) acrylate), polystyrene, and poly(methyl acrylate)-carrying pendent polymerizable caprolactone moieties were prepared by RAFT polymerization. The RAFT-made linear precursors were subsequently intramolecularly cross-linked at high polymer concentrations via organocatalyzed ROP using an alcohol initiator and methanesulfonic acid. While oligo(ethylene glycol) side chains were able to successfully form SCNPs, the other linear precursors resulted in multichain aggregates indicating the importance of side chain brushes in the formation of the SCNPs.

Single-chain polymeric nanoparticle formation based on functional precursor polymers can also be triggered by the controlled addition of bifunctional small molecules [91–98]. For example, Zhao and coworkers demonstrated the controlled self-assembly of amphiphilic monotailed SCNPs [99]. Poly(2-(dimethylamino)ethyl methacrylate)-block-polystyrene (PDMAEMA-*b*-PS) linear diblock copolymers with well-defined structures were synthesized by RAFT polymerizations. The quaternization reactions between PDMAEMA blocks and 1,4-diiodobutane (DIB) were employed in the preparation of monotailed SCNPs in 1,4-dioxane at very low polymer concentrations by slowly adding DIB to the solution. The cross-linking degree was controlled

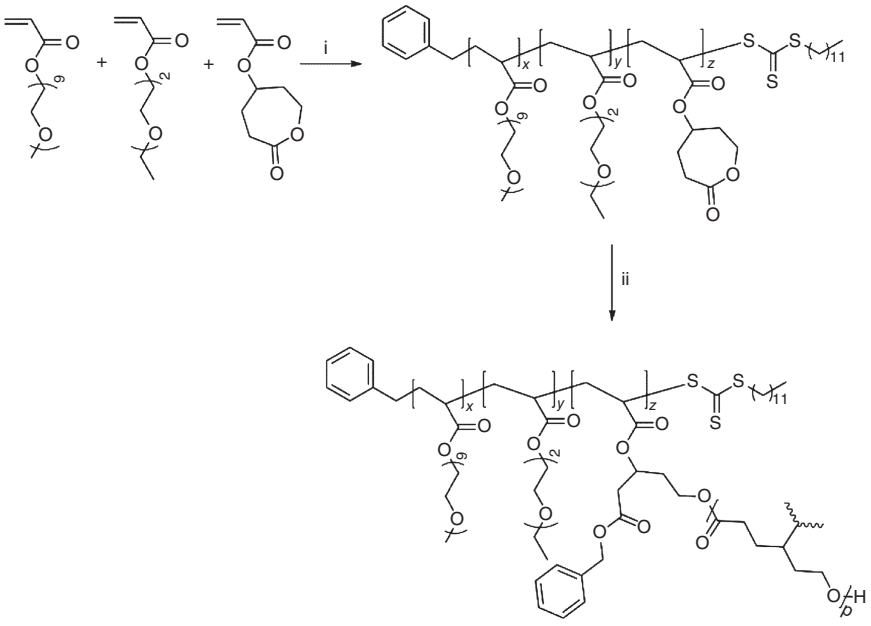

Figure 1.9 Collapse of single polymer chains to form monodisperse single-chain nanoparticles via intramolecular cross-linking mediated by ring-opening polymerization. (i) AIBN, RAFT agent, 80 °C. (ii) Benzyl alcohol as an initiator, methanesulfonic acid as an organocatalyst. (Wong *et al*. 2014 [90]. Reproduced with permission of the American Chemical Society.)

at 20%. As most DMAEMA units in the nanoparticles are not quaternized, the surface charge densities on the nanoparticles can be controlled by reaction of the SCNPs with varying amounts of iodomethane. With an increase in the charge density, the morphology of the aggregates in aqueous solutions changes from spherical micelles to vesicles to form a mixed morphology of wormlike cylinders and vesicles. The cross-linked SCNPs are observed by TEM and DLS. In interesting work demonstrating the effect of cross-linking agent dependency, the formation of water-soluble hydrophilic nanoparticles from biosynthetic poly-γ-glutamic acid (PGA) was described by Borbely and team [100]. PGA consists of repetitive glutamic acid units connected by amide linkages between α-amino and γ-carboxylic acid functional groups. The secondary structure of PGA has been described as α-helix in an aqueous solution. Nanoparticles were formed by cross-linking using 2,2′-(ethylenedioxy) diethylamine in the presence of water-soluble carbodiimide. The structure was determined by ^{1}H NMR and the particle size by TEM, SEC, and DLS measurements. The ratio of cross-linking agent was measured on the basis of the proton NMR spectra integrating the α-CH, β and β′-CH_2, and γ-CH_2 proton resonances. The results from TEM, SEC, and DLS reveal that the particle size depends on the ratio of cross-linking.

Importantly, Berda and coworkers reported controlled folding of a novel electroactive polyolefin via multiple sequential orthogonal intrachain interactions observing a large reduction in hydrodynamic volume [101]. Poly(oxanorbornene

anhydride-co-cyclooctadiene) was synthesized using ring-opening metathesis polymerization (ROMP) chemistry, where the anhydride groups along the backbone provides a reactive handle that can be readily decorated with a variety of nucleophiles, simultaneously inducing folding and installing functionality. An aniline tetramer was introduced providing electroactive properties and triggering the sequential folding process via supramolecular interactions. Next, the remaining anhydride groups were reacted with *p*-aminoaniline, serving to further fold the chain by pulling in the remainder of the oxanorbornene segments. Finally, the polycyclooctadiene segments are folded around the initial structure by connecting the olefins installed within the backbone during the ROMP using thiol–ene chemistry. The result is a tightly folded structure with a hydrodynamic volume that is 70% smaller than that of the original coil confirmed by a combination of SEC/MALLS and DLS.

1.4 Single-Chain Nanoparticles via Supramolecular Chemistry

Supramolecular chemistry is the chemistry of molecular assemblies and of intermolecular interactions in synthetic systems. It is dealing with chemistry beyond the molecule and highly selective interactions that occur between the partners, for example, a substrate binding to an enzyme. The α-helix and β-sheet structure of proteins rests on hydrogen bonds. Van der Waals interactions also play an important role in folded structures, since proteins are packed tightly and the close-range interactions dictate the structure of liquids and solids. Proteins assemble in a well-packed state, and the hydrophobic amino acids are located in the protein's core, while the polar amino acids are on the surface. This feature is obtained by hydrophobic interactions [29, 102]. Supramolecular non-covalent interactions used for single-chain folding in recent years are hydrogen bonds, host–guest systems, π–π interactions, metal complexation, and hydrophobic interaction [4, 25]. The commonly used functionalities and complementary motifs are presented in the following section.

The most prominent binding class for the realization of SCNPs are hydrogen bonds in the context of non-covalent interactions as introduced in the single-chain ring section of the current chapter. Several hydrogen bonding systems are known in literature to enable the formation of SCNPs. The benzene-tricarboxamide (BTA) is a well-studied example for hydrogen bonds in SCNPs technology [103–110]. For example, Meijer and coworkers showed in their studies that the BTA motif forms up to three hydrogens bonds and self-assembles in a helical manner in methylcyclohexane (MCH) [103–105]. The folding of the BTA unit can be controlled by attachment of a protected BTA moiety to the polymer chain [103]. The polymer was synthesized by copolymerization of a silyl-protected propargyl methacrylate (PMA) and isobornyl methacrylate (IBMA) in the ratio of 20 : 80 via the ATRP method to obtain a well-defined copolymer. Benzyl bromoisobutyrate initiated the polymerization with CuBr/tris(2-pyridylmethyl)amine(TPMA)/$Sn(EH)_2$ as catalyst for ARGET

ATRP. IBMA was copolymerized in order to enhance the solubility of the final polymer in aprotic solvents. The PMA was protected with a silyl group to prevent possible interactions of the alkyne with copper. The final polymer contains 25% propargyl groups. After quantitative deprotection, the BTA moiety was introduced to the propargyl group via a CuAAC reaction. Approximately half of the alkynes were functionalized to yield close to 20 BTA units per polymer chain. The overall molecular weight derived from SEC is 26 kg mol^{-1} and $Đ$ reads 1.7. After grafting of the BTA moiety, the UV-labile *o*-nitrobenzyl group was removed upon irradiation at a specific wavelength to control the folding ($\lambda = 354$ nm). The removal of the *o*-nitrobenzyl group was verified by ^{1}H NMR spectroscopy and results in the disappearance of the corresponding resonances in the NMR spectrum. After the cleavage of the nitrobenzene group, the polymer chain self-assembles into a helical shape. The synthesized polymer was insoluble in pure MCH. As a result, a mixture of dichloroethane and MCH (70 : 30) was used to dissolve the polymer, deprotect the BTA moieties, and induce excellent folding behavior. Temperature also plays an important role for the unfolding in reversible hydrogen bonding systems. The BTA unit remains unfolded at high temperatures (80 °C). By slowly decreasing the temperature, aggregation of the BTA units was observed. When a competitive solvent such as methanol is employed, hydrogen bond formation between the BTA units does not occur. The deprotection degree as well as the self-assembly of the BTA group was followed by circular dichroism (CD) and ultraviolet spectroscopy. As a result, the group of Meijer pioneered an ordered chiral SCNP. This feat makes the nanoparticle an excellent candidate for a possible catalytic system (Figure 1.10) [104].

In a related context, 2-ureidopyrimidinone (UPy) is a well-studied example in the field of single-chain folding, forming four hydrogen bonds [111–118]. Berda and colleagues synthesized a PMMA by SET-LRP with copper(0) and PMDETA as ligand [112]. MMA was copolymerized with a trimethylsilyl (TMS) protected alkyne-functional MA. The polymers contain 60% unfunctionalized MMA. Subsequently, the polymer was functionalized with the UPy folding motif by the CuAAC reaction. Polymers with varying degrees of conversion of the alkyne functionality were synthesized (30%, 50%, and 100% conversion of the alkyne). In order to control the folding, they protected the UPy moiety with the UV-labile *o*-nitrobenzyl group, which is photo-cleavable at 354 nm. In high dilution (1 mg ml^{-1}) SCNPs are existent, whereas larger aggregates assemble when higher concentrations are employed. After removal of the UV-labile protecting group, a shift to lower retention times in SEC data is observed, as the UPy dimerization leads to a reduced hydrodynamic diameter of the nanoparticle compared with the unfolded state. With increasing UPy content in the polymer, chain D_h increases, indicating the formation of more compact SCNPs, when the polymer chain features more functional groups for folding. This particular behavior is fundamental for single-chain folding and helps to better understand the characteristics of SCNPs. Further, AFM confirms the results obtained by SEC. After irradiation of the protected UPy polymer chains, the AFM-derived diameter of the formed particles decreased significantly, underpinning the SEC data.

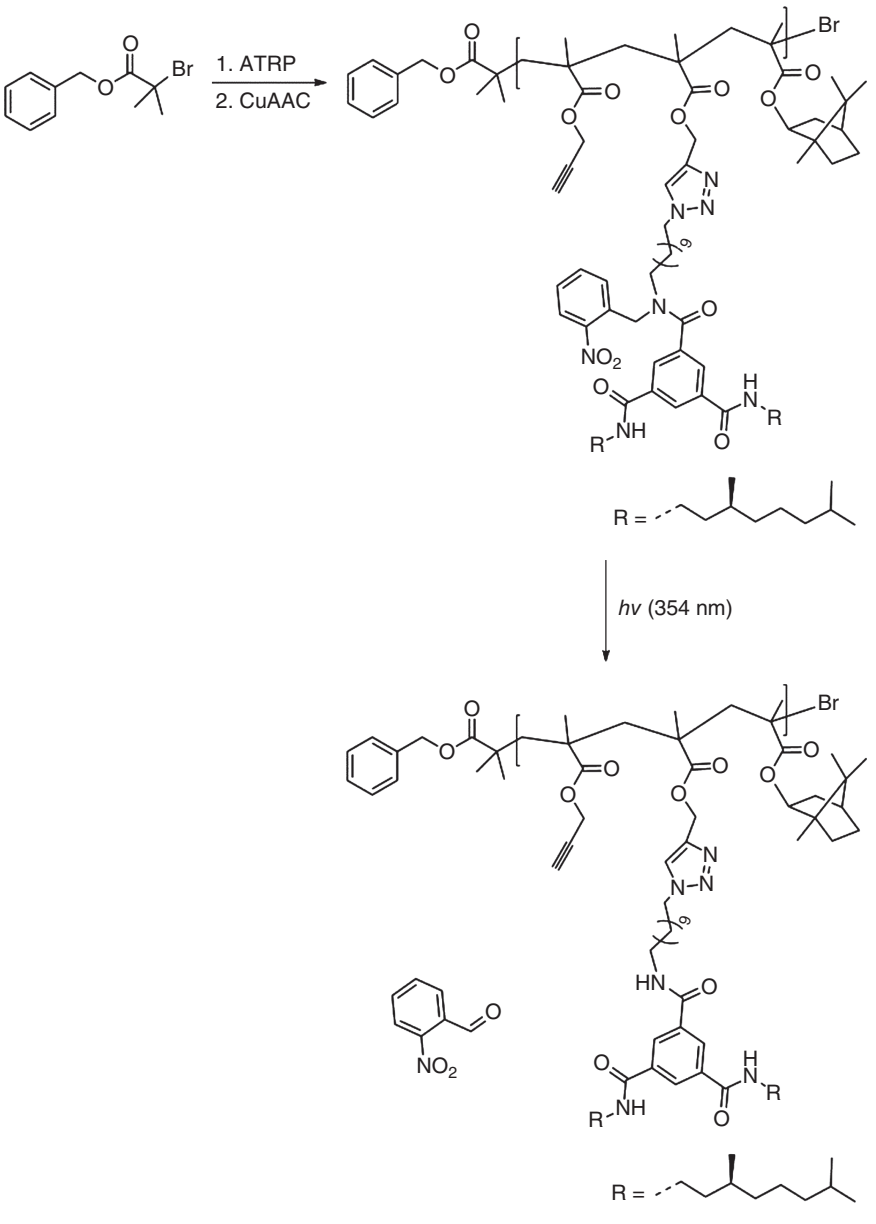

Figure 1.10 Chemical structures of polymers that can be intramolecularly self-assembled via triple hydrogen bonds under selected conditions generating helical structures employing ATRP and the CuAAC reaction. (Mes *et al*. 2011 [104]. Reproduced with permission of John Wiley and Sons.)

It is important to consider several types of hydrogen bonds to enlarge the toolbox of reversible SCNP folding technology. For example, Hawker and coworkers demonstrated the self-folding of the benzamide-containing polymer [116]. Furthermore, the concept of forming SCNPs using complementary hydrogen bonding interactions of ureidoguanosine (UG) and diaminonaphthyridine (DAN) was further explored by Weck and colleagues [117]. A UG-protected norbornene monomer, a DAN functional norbornene, and norbornene octyl ester (NOE) were copolymerized to obtain the triblock copolymer. First, the protected UG was polymerized, then the NOE spacer block was added, and last the DAN functional block was added. In the final block copolymer, the binding motifs UG–DAN are on the outer blocks A and C. Different ratios of monomer to initiator were employed (40 : 1, 60 : 1, 80 : 1 and 100 : 1) to afford polymers of 20, 23, 42, and 56 kDa with polydispersities of 1.78, 1.78, 1.39, and 1.63, respectively. The UG-protecting group was removed via dialysis in DMSO. The UG–DAN complementary motif provides yet another example exploiting four hydrogen bonds. At concentrations lower than 10 mM, single-chain folding is operational. The formation of hydrogen bonds in diluted systems was verified by ^{1}H NMR spectroscopy, resulting in a downfield shift of the resonances attributed to the protons involved in the hydrogen bonding process, as well as a broadening of the hydrogen bonding-associated UG proton resonances. The resulting SCNPs were additionally characterized by DLS, which underpins the formation of intermolecular aggregates at higher concentrations (50–30 mM), whereas at high dilutions (20–10 mM), SCNP formation is likely. The UG–DAN folding motifs enlarge the chemists' toolbox for hydrogen bond formation in SCNPs, which could lead to possible multiple orthogonally folded single-chain structures.

Inspired by the fact that an orthogonal folding strategy – that is, using two independently associating hydrogen bonding motifs – can be exploited for a two-step compaction process during SCNPs formation, it is possible to combine two recognition units and prepare a dual folding system as Hosono and colleagues demonstrated in their study [118]. An ABA-type triblock copolymer was synthesized with the BTA moiety on the B block and the UPy motifs attached to the A blocks. In an ATRP polymerization, PMA and hydroxyethyl methacrylate (HEMA) were copolymerized with IBMA to prepare postfunctionalizable polymers (poly(IBMA-*co*-HEMA)-block-poly(IBMA-*co*-PMA)-block-poly (IBMA-co-HEMA)). Initially, the B block – consisting of poly(IBMA-*co*-TMS-PMA) – was synthesized starting from a bifunctional ATRP initiator. The A blocks – poly(IBMA-*co*-TMS-HEMA) – were grown from the macroinitiator. After deprotection of the TMS-PMA block, the BTA motif was attached to the polymer via a CuAAC reaction, and the isocyanate functional UPy moiety was reacted with the hydroxyl functionalities on the A blocks. Polymers with molecular weights of 28.1, 52.6 124 kDa with polydispersities of 1.24, and 1.33 1.54 were prepared. The polymer (28.1 kDa) contains 3.8 alkynes and 6.4 OH groups per chain, the 52.6 kDa polymer has 6.3 triple bonds and 11.3 OH groups, and the 124 kDa polymer contains 16.6 alkynes and 27.9 OH groups per chain. The authors postulated orthogonality of the BTA self-assembly and the UPy dimerization. First, the BTA moiety self-assembled in a helical manner and subsequent deprotection of the UPy folding motif induced the dimerization

of the UPy recognition unit to result in a dual folded SCNP in high dilution (0.5 mg mL^{-1}). The orthogonality of the motifs was evidenced by ^{1}H NMR and CD spectroscopy, whereas the size and morphology of the generated structures was characterized by SEC, small-angle X-ray scattering (SAXS), and AFM. By lowering the temperature from 80 to 20 °C, a resonance shift in the NMR spectrum as well as broadening of the resonance, caused by protons attributed to the BTA moiety, was observed, indicating the BTA self-assembly. After UV irradiation, the benzyl proton resonances vanish and resonances assigned to the UPy dimerization are observed, while the BTA resonance remains intact. By heating the SCNP again to higher temperatures, the hydrogen bonds were broken again, indicating the orthogonality of the motifs as well as the reversibility of the chain folding. In CD spectroscopy, a maximum Cotton effect at $\lambda = 225$ nm was observed. In addition, the CD spectrum remained identical, suggesting that the deprotection of the UPy motifs does not affect the BTA self-assembly. SEC shows the characteristic shift of the retention time upon chain collapse in a noncompetitive solvent. SAXS measurements revealed a decrease of the radius of gyration from 14.4 to 11.1 nm, which is in agreement with the shift observed by SEC. In AFM measurements, the partly folded (BTA-assembled) particle is visualized as well as the fully folded (deprotected) UPy moiety. The difference between the partly and fully collapsed states is visualized in a more compact shape of the fully collapsed nanoparticle compared with the partly collapsed analog. Such dual folded systems constitute a step toward natural proteins, since they have multiple bonding sites.

In 1988, Hamilton and coworkers developed a molecular recognition unit consisting of the so-called HW and CA. These particular recognition units form six hydrogen bonds [119]. In 2006, Hager and colleagues made use of the HW–CA recognition motif in the field of supramolecular dendrimer chemistry [120, 121], whereas Barner-Kowollik and coworkers transferred the folding motif to the field of single-chain folding to construct a dual orthogonal folding system together with the Meijer group (Figure 1.11) [122]. Recently, the Meijer and Barner-Kowollik groups shared their respective expertise on the BTA and HW–CA folding motifs, resulting in a dual folding system, going one step further in mimicking natural proteins. For this purpose, a triblock copolymer system was synthesized via RAFT polymerization based on variable-functionalized MMAs. For the first block, 2-ethylhexyl methacrylate (EHMA) was copolymerized with a primary alkyl bromide-bearing MA. The commercially available CTA 4-cyano-4-((phenyl-carbonylthioyl)thio)pentanoic acid was esterified with ethanol and subsequently used as RAFT agent and AIBN as initiator for the polymerization. The ratio of EHMA/bromine-functional methacrylate/CTA was selected to be 190 : 10 : 1. For the second block, the macro-CTA was copolymerized with EHMA and a silyl-protected PMA (ratio = 190/10 : 1). For the last block, the macro-CTA was copolymerized again with EHMA and a silyl-protected HEMA. The resulting triblock copolymer contains close to 5% of each functional monomer. Before the folding motifs were attached, the CTA end group was removed in a radical-induced reaction, due to possible side reactions during the CuAAC reaction. The HW–CA moieties were orthogonally linked to the outer blocks A and C in post-polymerization modifications (etherification

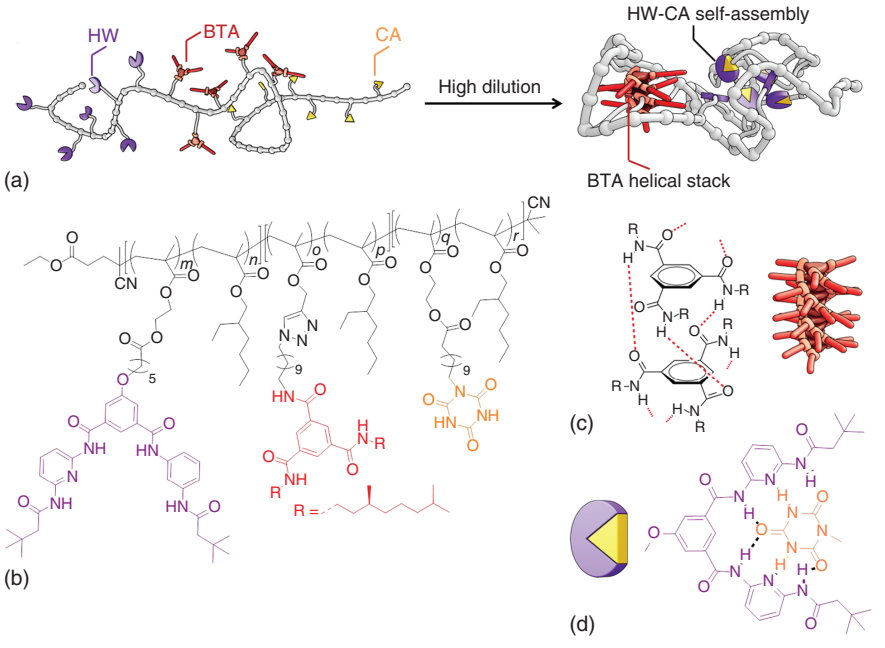

Figure 1.11 (a) Design of a triblock copolymer with orthogonal complementary motifs (HW, BTA, and CA) alongside the polymer chain, which is designed to fold into a compartmentalized structure via orthogonal self-assembly. (b) Chemical structure of the functionalized triblock copolymers. (c) Self-assembly of BTA units via threefold symmetric hydrogen bonding. (d) Self-assembly of HW and CA via multiple hydrogen bonding. (Altintas *et al*. 2015 [122]. Reproduced with permission of the American Chemical Society.)

and esterification), while the BTA motifs were attached to the middle block B via CuAAC.

The BTA and HW–CA moieties self-assemble orthogonally in high dilution (1 mg mL^{-1}). The BTA moieties self-assemble helically, whereas the HW–CA ones assemble statistically without a preferred configuration. The resulting SCNP provides some controlled conformation. Interaction and orthogonality of the complementary motifs was characterized by ^{1}H NMR. The BTA moieties result in a broad resonance at 6.45 ppm. Resonances at 12.72, 9.75, and 9.36 ppm indicate the HW–CA interaction. Together with temperature-dependent CD spectroscopy, where the CD spectrum clearly indicated the folding of the BTA units upon cooling the solution from 90 to 5 °C, the orthogonality of the folding motifs was demonstrated. D_h obtained by DLS were 11.7 and 24.4 nm, depending on the molecular weight (51.4 and 85.1 kDa) with about 5 mol% of each motif in the polymer.

The crown ether–secondary ammonium salt (AS) recognition motif is commonly used in supramolecular chemistry [123–127]. Barner-Kowollik and coworkers transferred this binding principle to the field of single-chain folding (refer to Figure 1.12) [128]. In order to demonstrate its power and applicability in single-chain technology, an AB-type diblock copolymer system was prepared based on different functionalized MMA monomers (bromine-functional MA and

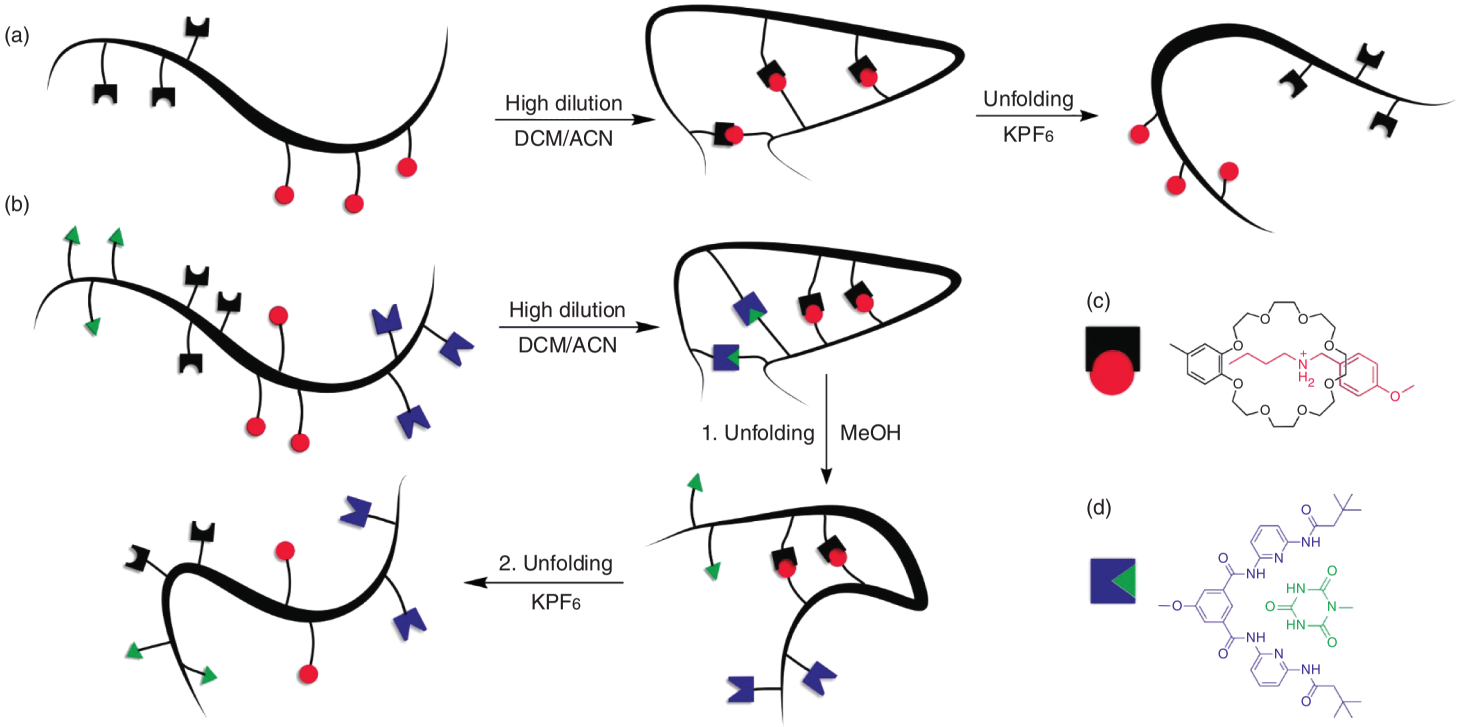

Figure 1.12 (a) Design of the initial diblock copolymer system bearing the host–guest folding motif (B21C7/AS), followed by the folding/unfolding of the resulting SCNP. (b) Design of the tetrablock copolymer systems featuring the orthogonal complementary folding motifs (HW/CA and B21C7/AS), followed by folding and the orthogonal stepwise unfolding. (c) Self-assembly of HW and CA via multiple hydrogen bonds. (d) Self-assembly of B21C7 and AS units via host–guest complexation. (Fischer *et al*. 2016 [128]. Reproduced with permission of John Wiley and Sons.)

TMS-protected alkyne-functional MA copolymerized with EHMA) in a proof-of-principle study. Ethyl 4-cyano-4-((phenylcarbonothioyl)thio)pentanoate was used as the CTA and AIBN as the radical source. In the first block, 5 mol% of the bromine functionality was incorporated. For the second block, the macro-CTA was copolymerized with EHMA and the TMS-protected alkyne-functional MA. The alkyne functionality was found to be close to 6.5 mol%. In a post-polymerization modification, the benzo-21-crown-7 (B21C7) host and the secondary AS guest were linked to the polymer orthogonally by etherification and CuAAC, respectively. The molecular characteristics of the precursor were $M_n = 30.6$ kDa and $Đ = 1.1$. The formed SCNPs as well as the subsequent unfolding of the particles were characterized by DLS and DOSY. The addition of a potassium salt to disrupt the host–guest interaction lead to a significant increase in the DLS- and DOSY-derived D_h. Importantly, a dual folding system consisting of the HW–CA hydrogen bond pair as well as the B21C7-AS motif was prepared. Wang and coworkers already showed the orthogonality of the system in their work in the field of supramolecular chemistry [54]. For this dual folding system, an ABCD-type tetrablock copolymer was synthesized with different functional MMA-based monomers via RAFT and subsequent orthogonal attachment of the folding motifs. For the first block, the bromine-functional MA was copolymerized with EHMA using AIBN and the same CTA as for the diblock copolymer. For the second block, the TMS-protected alkyne-functional MA was copolymerized with EHMA and the macro-CTA. In the third block, the macro-CTA was copolymerized with EHMA and a TMS-protected alkyne-functional MA, resulting in a triblock copolymer. In the last block, the macro-CTA was copolymerized with EHMA and a triisopropysilyl (TIPS)-protected hydroxyl-functional MA giving the final precursor tetrablock copolymer. The precursor tetrablock copolymer contains 5 mol% of the bromine-functional MA, 5.5 mol% of the TMS-protected alkyne, 6 mol% of the TIPS-protected alkyne, and 2.4% of the TMS-protected hydroxyl functionality. The HW–CA recognition units were placed within the outer blocks A and D via etherification and Steglich esterification, respectively. The host–guest systems were attached orthogonally to the inner block B and C through CuAAC. The overall molecular weight of the tetrablock copolymers was close 64.8 kDa ($Đ = 1.2$).

These authors demonstrated that the folding units assemble orthogonally and can be unfolded stepwise in an orthogonal, pathway-independent manner. Both SCNP systems (AB and ABCD type) occur in high dilution (2.5 mg mL^{-1}) in a noncompetitive solvent such as chloroform or dichloromethane. By addition of a competitive solvent such as methanol, the hydrogen bonds are disrupted, and the addition of KPF_6 leads to decomplexation of the host–guest system. The inversion of the trigger signal addition leads essentially to the same results. This study pioneers the control over orthogonal stepwise unfolding of dynamic SCNPs by external chemical stimuli, constituting a critical step toward understanding the folding/unfolding behavior of SCNPs.

It is important to investigate various types of binding motifs due to the fact that nature uses not just (reversible) hydrogen bonds complex for biomolecule design. An important class of motifs that are introduced for single-chain

folding are host–guest systems [129, 130]. A further host–guest system is cucurbit[*n*]uril (CB[*n*]; $n = 5–8, 10$) with a hydrocarbon motif. Cucurbit[*n*]uril consists of several glycoluril units, where *n* is the number of units [131]. For example, CB[8] consists of eight glycoluril units. The CB moiety is functioning as host system and can simultaneously bind two hydrocarbons, for example, two aromatic molecules such as biphenyl or naphthyl analogs [132]. Appel *et al*. [133] synthesized a water-soluble poly(*N*-hydroxyethyl acrylamide) via ATRP with molecular weights from 133 to 440 kDa with $Đ$ from 1.15 to 1.24. The aromatic motifs – a substituted bipyridine and a substituted naphthyl moiety – were attached in post-polymerization reactions to the hydroxyl functionalities via isocyanate coupling. Subsequently, CB[8] was added to a solution of the polymer and SCNPs formed. The nanoparticles are generated rapidly, show reversibility, and are highly tuneable. A maximum cross-linking degree of 15% was achieved, indicating saturated CB[8] moieties. DLS evidenced the characteristic decrease of D_h as a result of the collapse. The concentration for the formation of particles was close to 0.1 mg mL^{-1} (refer to Figure 1.13). The host–guest interaction was also evidenced by ^{1}H NMR spectroscopy via downfield shifts of the aromatic protons of the naphtyl moiety upon SCNP formation. Moreover, the UV/Vis

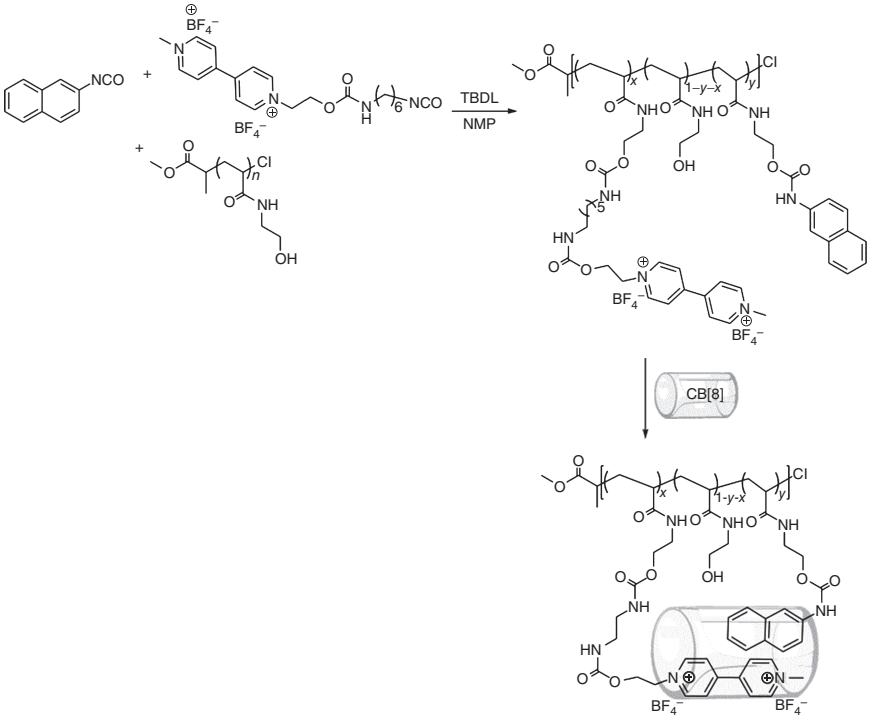

Figure 1.13 Decoration of a poly(*N*-hydroxyethyl) acrylamide homopolymer with bipyridine and naphthyl moieties via isocyanate coupling and subsequent SCNP formation through host–guest complexation after the addition of cucurbit[8]uril (CB[8]) cross-linker in high dilution (0.1 mg mL^{-1}). (Appel *et al*. 2012 [133]. Reproduced with permission of John Wiley and Sons.)

spectrum showed a peak at 521 nm associated with a charge transfer complex of the cross-linked host–guest complex. Decomplexation can be caused by different stimuli, such as pH, light, and temperature. Importantly, these reactions are feasible in water.

Furthermore, folding of single polymer chains to form SCNPs is possible via the interaction of two aromatic blocks in the polymer chain in the context of π–π interactions. Weck and coworkers successfully synthesized a β-hairpin-folded polymer, making the resulting SCNP highly interesting because of its controlled structure (Figure 1.14) [134]. The polymer consists of three blocks, that is, a pentafluorostyrene (PFS) block, a *N*,*N*-dimethylacrylamide middle block, and a styrene block. The polymer was synthesized via RAFT polymerization, using 4-cyano-4-((phenylcarbonothioyl)thio)pentanoic acid as RAFT agent and AIBN as radical initiator. The triblock copolymer was prepared by sequential polymerization of styrene, *N*,*N*-dimethylacrylamide, and 2,3,4,5,6-pentafluorostyrene. The molecular characteristics are $Đ = 1.73$ with an apparent molecular weight of 20.8 kDa. Here, the folding occurs between two aromatic rings via π–π interaction resulting in a β-hairpin-folded conformation. Styrene is electron rich, whereas PFS is electron deficient. The solvent plays an important role with regard to the folding. Since toluene is a competitive solvent and can inhibit the interaction of styrene with PFS, a noncompetitive solvent such as DMF leads to the folded polymer. Another requirement for folding a polymer is to

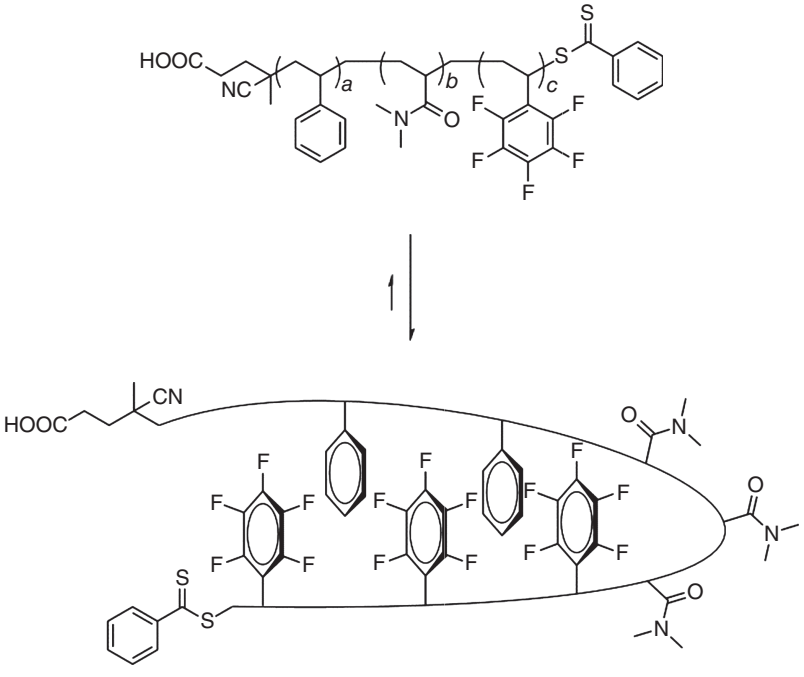

Figure 1.14 Single-chain folding of the PS_{30}-*b*-$PDMAA_{20}$-*b*-$PPFS_{30}$ block copolymer into a β-hairpin-folded SCNP via π–π-interactions. (Lu *et al.* 2014 [134]. Reproduced with permission of the Royal Society of Chemistry.)

avoid intermolecular interactions, which would lead to higher D_h obtained by DLS. In chloroform, intramolecular interactions occur until a concentration of 50 mg mL^{-1}. Additionally, the folding of the polymer was confirmed by 2D NMR spectroscopy (NOESY and HOESY), showing a strong NOE between the aromatic protons of the PS block with the polymer backbone of the PPFS block at 6.65, 2.07, 1.98, and 1.38 ppm. In benzene, one NOE resonance is observed, indicating the interaction of the aromatic protons of PS with the PS backbone. As a result, the PS–PFS interaction is inhibited. HOESY experiments indicate the *ortho*-F of the PFS moieties along the PPFS block gives several HOE resonances with the backbone protons of PPFS and PS at −162 and 1.7 ppm, indicating a quadruple interaction. Again, in toluene no quadruple interactions are observed in HOESY measurements.

Inspired by the metal–ligand interactions of natural proteins, many researchers focus on the preparation of SCNPs via these interactions [135–142] as well as their applications as catalytic systems, which are further discussed in Chapters 6 and 9 of the present book, respectively. However, two examples of metallo-containing single-chain polymer nanoparticles are presented here, including the metals Cu and Pd. For example, the group of Paik prepared SCNPs by the intramolecular formation of copper phthalocyanines (CuPcs) (refer to Figure 1.15) [143]. These authors synthesized polystyrene-co-poly[4-((4-vinylbenzyl)oxy)phthalonitrile] via the RAFT polymerization process using AIBN and CPBD. Cyclotetramerization in benzyl alcohol led to the formation of SCNPs upon the addition of CuCl salt and phthalonitrile. Polymers with different percentages of 4-((4-vinylbenzyl)oxy)phthalonitrile (VBOP) were prepared to demonstrate possible differences in the nanoparticle formation. Here, copolymers with 3, 9, and 17 mol% VBOP were synthesized. As a result, with increasing VBOP content, the SEC-derived D_h decreased after the cyclotetramerization. The shift of the retention time to higher elution volume is an indication for the successful formation of SCNPs. The formation of CuPcs in the nanoparticles was followed by FT-IR. The disappearance of the cyano group band at 2230 cm^{-1} and the new band of the imine group at 1720 cm^{-1} suggest the successful formation of

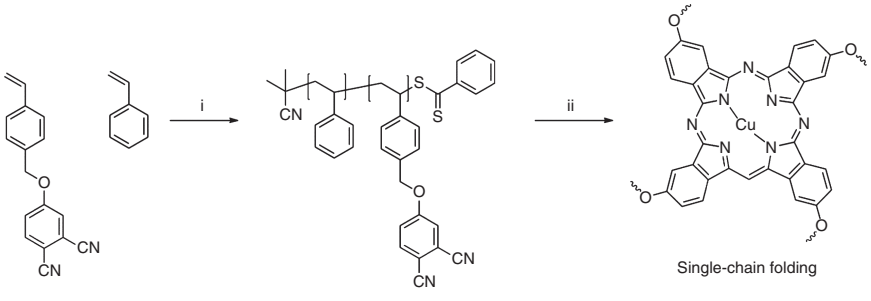

Figure 1.15 Synthesis of the polystyrene-*co*-poly[4-((4-vinylbenzyl)oxy)phthalonitrile] via RAFT polymerization and the subsequent formation of SCNPs by cyclotetramerization. (i) AIBN, DMF, CPBD, 65 °C. (ii) Phthalonitrile, CuCl, DBU, benzyl alcohol, 150 °C, 29 h. (Jeong *et al*. 2015 [143]. Reproduced with permission of the Royal Society of Chemistry.)

CuPcs. The number of incorporated CuPcs in the nanoparticle was calculated from UV–vis spectra. For 3 mol% copolymer, 3.4 CuPcs in the nanoparticle were estimated. For the 9 and 17 mol% copolymers, the calculation revealed an incorporation of 7 CuPcs in the corresponding nanoparticles. Both copolymers contain the same amount of CuPcs, which is due to the lack of sufficient free volume to build CuPcs in the collapsed nanoparticle. In this study, copper is complexed by nitrogen compared with the work by Pomposo where copper is complexed by carbonyl functionalities [143]. In addition, successful SCNP formation was evidenced by optical inspection due to a change of the mixture from a dark brown (unfolded) to bluish green for the folded SCNP.

Barner-Kowollik and coworkers pioneered the Pd-complex-driven formation of SCNPs (Figure 1.16) [137]. In the associated study, well-defined SCNPs cross-linked by palladium (II) complexes are introduced using the repeating-unit approach. The precursor polymer was synthesized by copolymerization of styrene and 4-(chloromethyl)styrene via NMP and the subsequent attachment of triarylphosphine ligand moieties to the chloromethyl functional monomer in an esterification ($M_n = 12.3$ kDa, $Đ = 1.16$). The amount of functional monomer in the polymer was estimated to be close to 12 mol%, which was fully converted with the triarylphosphine ligand moieties. The collapse was induced at high dilution (4 mg mL^{-1}) by dichloro(1,5-cyclooctadiene)palladium(II) ([Pd(COD)Cl$_2$)]), since the COD ligand is an excellent leaving group in the ligand exchange reaction with triarylphosphine species. For SCNP formation, the functionalized polymer was dissolved in DCM and added dropwise to a solution of the palladium ligand. The highest degree of cross-linking was reached with a ratio 1 : 2 of the cross-linker to ligand. The formation of the SCNPs was evidenced by SEC and DLS, which both show a significant decrease of the hydrodynamic diameter after folding. The DLS-derived D_h decreases from 8.8 nm before cross-linking to 5.4 nm after the SCNP collapse. NMR spectroscopy based on hydrogen and phosphorous supported the cross-linking. Specifically, the proton resonances of the triarylphosphine groups shift to lower field, the phosphor resonance in the ^{31}P spectrum shifts from −5.06 ppm (uncomplexed) to 23.54 ppm (complexed), indicating quantitative coordination. The configuration of the Pd complexes is probably trans, since the conformation is dependent on the cone angle of the ligands in [Pd(PR$_3$)Cl$_2$] and the polymer forms large rings. [64] ^{1}H spin–spin relaxation times (T_2) provide additional information regarding the intramolecular cross-linking. When the SCNP is formed, T_2 decreases from 147 to 70 ms, because of the reduced mobility of the chain segments. In a proof-of-concept study, the Pd-containing SCNP was also shown to catalyze the Sonogashira coupling of terminal alkynes and aryl halides. By using palladium as a cross-linker, a variety of other chemical reactions are possible to be catalyzed by the SCNP, yet the full scope for catalysis still has to be explored.

A final class of SCNPs to consider is those collapsed by non-covalent hydrophobic interactions. Such SCNPs have been, for example, introduced by the group of Sawamoto [144–146]. Synthetically, a series of water-soluble methacrylate-based amphiphilic copolymers were synthesized by ruthenium-catalyzed RDRP. Poly(ethylene glycol) methyl ester methacrylate (PEGMA) was copolymerized

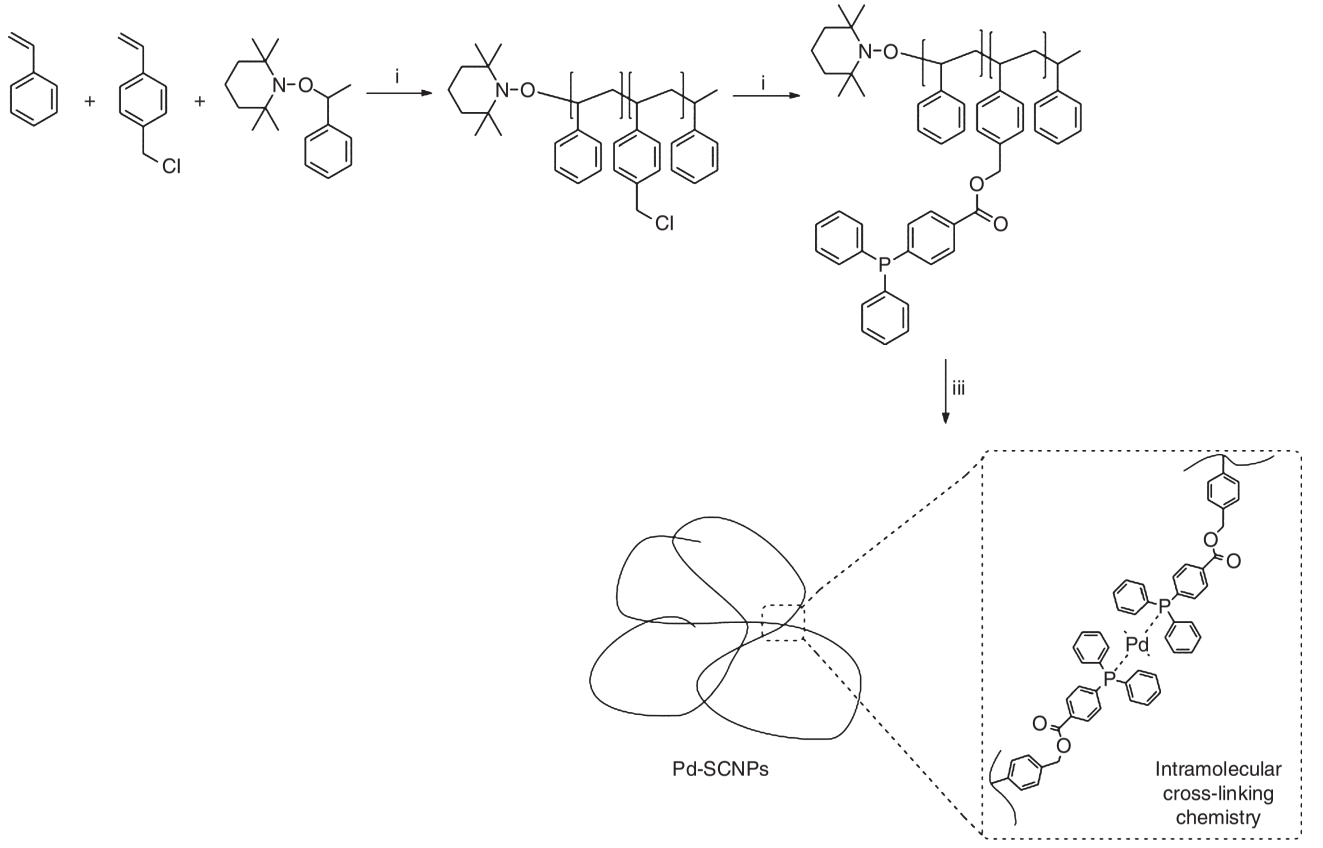

Figure 1.16 Synthetic strategy for the preparation of palladium(II)-cross-linked single-chain nanoparticles (Pd-SCNPs). (i) Bulk, 125 °C, 5 h. (ii) 4-(Diphenylphosphino)benzoic acid, K_2CO_3, DMF (dry), 50 °C, 16 h. (iii) $Pd(COD)Cl_2$, DCM (dry), r.t., 21 h. (Willenbacher *et al.* 2015 [137]. http://pubs.rsc.org/-/content/articlehtml/2015/py/c5py00389j, Used under CC BY 3.0 https://creativecommons.org/licenses/by/3.0/.)

with alkyl methacrylates (RMA) such as MMA, *n*-butyl methacrylate (*n*-BMA), *tert*-butyl methacrylate (*t*-BMA), *n*-octyl methacrylate (OcMA), dodecyl methacrylate (DMA), 1-adamantylethyl methacrylate (AdMA), cyclododecylmethyl methacrylate (CDMA), and octadecyl methacrylate (ODMA) (Figure 1.17) [144]. PEGMA was randomly copolymerized with RMA, using [Ru(Ind)Cl-$(PPh_3)_2$/*n*-Bu_3N] as catalyst and ethyl-2-chloro-2-phenylacetate as chloride initiator. The ratio of PEGMA to RMA was in the range of 200/0–80/120, 80/20. The well-defined polymers ($M_n = 36.1$–54.4 kDa) feature narrow molecular weight distributions ($Đ = 1.2$–1.4). The folding was characterized by SEC/MALLS and DLS. In case the polymer folds intramolecularly by hydrophobic interactions, its molecular weight in water should be identical to the value estimated as that of a single chain, while the size should decrease in water compared with that in good organic solvents. SEC-MALLS measurements were performed in water and DMF. In DMF, M_n ranges from 70.3 to 143.8 kDa, which is in agreement with the calculated M_n from NMR. The association number, which is defined as the ratio of $M_{w\,(DMF,MALLS)}$ to $M_{w,calcd}$, is almost 1, indicating the formation of single-chain aggregates in DMF by the amphiphilic polymers. In water, $M_{w\,(MALLS)}$ ranges from 71.2 to 491.6 kDa. Therefore, the association number varies from 1 to 5. Note that the hydrophobicity of RMA is not always the same. The DMA copolymer with 40 mol% DMA (PEGMA/DMA = 200/0–120/80, 80/20) shows unimer formation, and with increasing DMA content (50 mol% or more), intermolecular aggregates are formed, due to an association number larger than 2. All RMA polymers with 20 mol% RMA content display single-chain aggregation, independent of the hydrophobic structure and degree of polymerization. As a result, the intra- or intermolecular interactions are dependent on the local concentration of RMA content. DLS measurements were performed in different solvents. In water, the hydrodynamic radium (R_h) decreases with increasing RMA content until 40 mol% of RMA in the copolymer; with further increasing RMA content (50 mol%), R_h increased indicating intermolecular interaction above 50 mol% RMA. The steric repulsion by the hydrophilic PEG chains and the intramolecular hydrophobic interaction from the RMA moieties isolate the single chain in water to prevent intermolecular interactions. Therefore, the compact structure of the polymers in water was visible even in high concentrations (up to 60 mg mL^{-1}) and at high temperatures (from 25 to 80 °C). In organic solvents (DCM and DMF), R_h remained constant, indicating independent conformation of the copolymer in good organic solvents. The polymers with 20 mol% RMA content generally show a smaller R_h in water compared with the R_h obtained by measurements in DCM. The comparison of the peak-top molecular weight (M_p) in water and DMF leads to the conclusion that the folded structure of the polymers with increasing hydrophobicity becomes more compact, due to a decreasing value for the ratio of $M_{p(water)}/M_{p(DMF)}$ (minimum value is 0.5). The high concentration for the formation for SCNPs as well as the natural medium – water – pushes SCNP technology one step further in the direction of mimicking natural macromolecules, such as proteins.

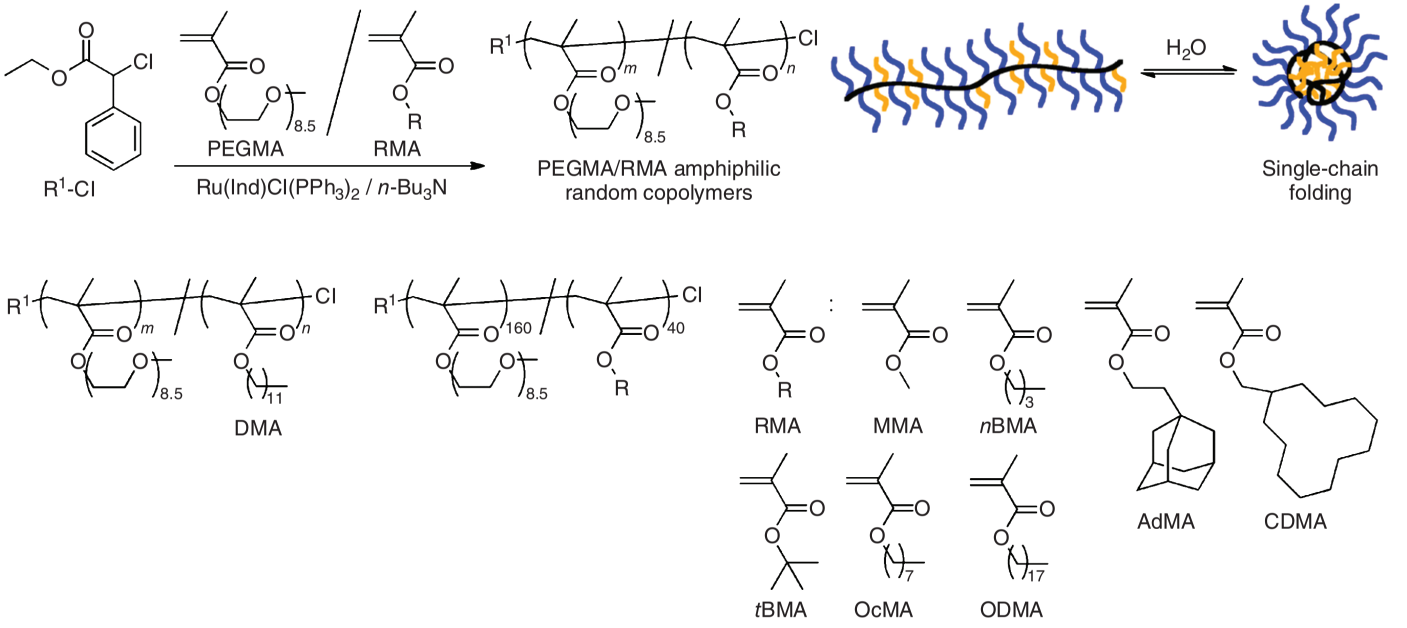

Figure 1.17 Synthesis of different poly(PEGMA-*co*-RMA) amphiphilic random copolymers via ruthenium-catalyzed living radical polymerization and schematic illustration of the single-chain folding of these amphiphilic copolymers in water. (Terashima *et al.* 2015 [144]. Reproduced with permission of the American Chemical Society.)

1.5 Single-Chain Nanoparticles Based on Dynamic Covalent Chemistry

Dynamic covalent chemistry (DCC) addresses reversible covalent reactions that allow the formation of reversible covalent bonds under thermodynamic control to generate dynamic combinatorial libraries [147, 148]. Orthogonal dynamic covalent bonds are of interest for the construction of functional systems combining the characteristics of covalent and non-covalent bonds [149]. DCC continuously gained importance in the field of SCNPs as it is a very valuable addition to the SCNP toolbox [150–153]. The most popular pair of orthogonal dynamic bonds, hydrazones and disulfides, exchange exclusively under acidic and basic conditions, respectively, and thus enable the construction and operation of various "dual dynamic functional systems [154, 155]. For example, Fulton and coworkers presented the preparation of polymeric nanoparticles through the chain collapse of linear polymers driven by the formation of dynamic covalent bonds [156]. Poly (vinylbenzaldehyde) (PVBA) was prepared by RAFT polymerization yielding linear polymers with aldehyde functionalities along the backbone. Linear chains of PVBA were intramolecularly cross-linked by dropwise addition of a cross-linker (bis-hydrazide) with various quantities in THF followed by addition of a catalytic amount of TFA. The degree of cross-linking was controlled by varying the amount of cross-linker. Further functionalization of the resulting nanoparticles was achieved by reaction of their remaining aldehyde groups with monoacyl hydrazides or alkoxyamines that provide potential applications for the nanoparticles. The functional polymeric nanoparticles were characterized by SEC, ^{1}H NMR spectroscopy, and DLS. The SEC trace of the linear polymers systematically shifted to low molecular weight regions, indicating the folding of the single polymer chains as a result of the reduction in their hydrodynamic volume. In interesting work with a promising potential application, Thayumanavan and colleagues reported a facile approach to form SCNPs via disulfide-based intrachain cross-linking of single polymer chains of a random copolymer [157]. The random copolymer Poly(HEMA-*co*-PDSEMA) of 2-HEMA and pyridyl disulfide (PDS) ethyl methacrylate (PDSEMA) was synthesized by RAFT polymerization. The PDS groups were cleaved to generate a reactive thiol unit in the polymer upon addition of the D,L-dithiothreitol (DTT). Subsequently, the thiols react with the remaining PDS units to produce SCNPs which were characterized by ^{1}H NMR, AFM, DSC, SEC, and DLS. The reduced segmental mobility of the cross-linked SCPNs has a significant impact on the glass transition temperature (T_g). For instance, the T_g value gradually increased from an initial value of 76 °C for the precursor polymers to 110 °C for SCNPs based on DSC measurements, showing a decrease in segmental chain mobility with increasing cross-linking density. The influences of the cross-linking density were additionally investigated, indicating that more compact SCNPs were obtained by increasing the cross-linking density. In addition, the size of the SCNPs was tuned by varying the molecular weight of the precursor polymers. The specifically redox-responsive nature of these SCPNs makes these SCNPs useful for specific applications, for example, in

drug delivery. In related work, Pomposo and coworkers reported the synthesis of ultrasmall PMMA nanoparticles by the metal-free cross-linking of linear chains at ambient temperatures [158]. The precursor copolymers of MMA and (2-acetoacetoxy)ethyl methacrylate (AEMA), containing different molar fractions of the β-ketoester-reactive group, were synthesized by RAFT polymerization using CPDB and AIBN. The intramolecular collapse was performed by the one-pot reaction of the β-ketoester moieties with alkyl diamines in tetrahydrofuran. The collapsing process upon enamine formation was followed by SEC, FT-IR, and ^{1}H NMR spectroscopy. The size of the resulting polymeric nanoparticles was determined by DLS. Enamine ligation chemistry increases the synthetic toolbox for the efficient synthesis of metal-free, ultrasmall dynamic SCNPs.

1.6 Conclusions and Outlook

While nature's degree of control for the synthesis in biomacromolecules remains unreached by synthetic macromolecular chemistry, significant progress into mimicking molecules such as proteins and enzymes on the basis of synthetic polymers has been made. Single-chain folding technology based on covalent bonds and non-covalent interactions has grown significantly and rapidly in recent years and features high potential for biomimetic applications, precision catalytic systems, or sensor materials. Covalent bonds and non-covalent interactions and dynamic covalent bonds have been exploited, which are also nature's choice for stabilizing its globular functional structures. Several modular ligation reactions such as alkyne–azide cycloaddition, alkyne homocoupling, thiol-ene chemistry, Michael addition, amide formation, tetrazine–norbornene coupling, nitrile–imine ene ligation, thiol–yne chemistry, photodimerization of anthracene, metal complexation, photo-cross-linking of azides, and photoenols have been exploited to synthesize complex folded entities. The most popular pair of orthogonal dynamic bonds, hydrazones and disulfides, exchange exclusively under acidic and basic conditions and thus enable the construction and operation of various dual dynamic functional systems. SCNPs based on non-covalent interactions such as hydrogen bonds, π–π stacking, host–guest systems, hydrophobic interactions, and metal complexation have been realized, which are also used by nature to dynamically change the morphology of its biocatalysts. One of the most recent examples of a dual-gated reversibly folded SCNP system comes from our team, where the limits of folding point orthogonality have been pushed by exploiting host–guest systems and hydrogen bonding in one SCNP system [128]. Such reversibly non-covalently folded polymers provide a glimpse of what may be possible in terms of gating SCNP folding.

In summary, several folding motifs are well established, studied, and exploited in initial attempts to synthesize structures that are mimicking – on a simple level – the functionality observed in biomacromolecules. Further, first examples of functional dual folding systems are emerging. Critically, the SCNP community must now focus on combining folding motifs orthogonally to construct complex

SCNP systems, able to respond to adapt to their environment in response to orthogonal outer signals and – most importantly – remaining functional over extended periods of time when carrying out a specific task, for example, as a (bio)catalyst [159]. Ultimately, SCNPs need to function in aqueous environments, and thus strategies are required that allow for their gated folding and unfolding in such regimes, finally with full control over their exact morphology. In terms of shaping exact morphologies, the advent of sequence-defined polymers will play a crucial role. Analytically, the folding and unfolding processes that govern SCNPs need to be able to allow for a "live" dynamic molecular vision of folding and unfolding processes, and we submit that especially nuclear resonance techniques that are currently well established in the realm of protein analysis need to be translated into the realm of SCNPs.

Acknowledgments

C.B.-K. acknowledges continued support for his team's work on advanced SCNP systems in the context of the Sonderforschungsbereich 1176 funded by the German Research Council (projects A1, A2, and A3) as well as the Queensland University of Technology (QUT).

References

1 Anfinsen, C.B. (1973) Principles that govern the folding of protein chains. *Science*, **181** (4096), 223–230.
2 Branden, C.T.J. (1998) *Introduction to Protein Structure*, Garland Publishing, New York.
3 Dobson, C.M. (2003) Protein folding and misfolding. *Nature*, **426** (6968), 884–890.
4 Altintas, O. and Barner-Kowollik, C. (2012) Single chain folding of synthetic polymers by covalent and Non-covalent interactions: current status and future perspectives. *Macromol. Rapid Commun.*, **33** (11), 958–971.
5 Lutz, J.-F., Ouchi, M., Liu, D.R., and Sawamoto, M. (2013) Sequence-controlled polymers. *Science*, **341** (6146), 1238149.
6 Sanchez-Sanchez, A., Pérez-Baena, I., and Pomposo, J. (2013) Advances in click chemistry for single-chain nanoparticle construction. *Molecules*, **18** (3), 3339.
7 Kuhn, V.W. and Majer, H. (1956) Die selbstvernetzung von fadenmolekülen. *Makromol. Chem.*, **18** (1), 239–253.
8 Kuhn, W. and Balmer, G. (1962) Crosslinking of single linear macromolecules. *J. Polym. Sci.*, **57** (165), 311–319.
9 Longi, P., Greco, F., and Rossi, U. (1968) Polyolefins containing intra-molecular crosslinks. *Makromol. Chem.*, **116** (1), 113–121.
10 Braunecker, W.A. and Matyjaszewski, K. (2007) Controlled/living radical polymerization: features, developments, and perspectives. *Prog. Polym. Sci.*, **32** (1), 93–146.

11 Ouchi, M., Terashima, T., and Sawamoto, M. (2009) Transition metal-catalyzed living radical polymerization: toward perfection in catalysis and precision polymer synthesis. *Chem. Rev.*, **109** (11), 4963–5050.

12 Moad, G., Rizzardo, E., and Thang, S.H. (2009) Living radical polymerization by the RAFT process – a second update. *Aust. J. Chem.*, **62** (11), 1402–1472.

13 Gregory, A. and Stenzel, M.H. (2012) Complex polymer architectures via RAFT polymerization: from fundamental process to extending the scope using click chemistry and nature's building blocks. *Prog. Polym. Sci.*, **37** (1), 38–105.

14 Nicolas, J., Guillaneuf, Y., Lefay, C., Bertin, D., Gigmes, D., and Charleux, B. (2013) Nitroxide-mediated polymerization. *Prog. Polym. Sci.*, **38** (1), 63–235.

15 Meldal, M. and Tornøe, C.W. (2008) Cu-catalyzed azide–alkyne cycloaddition. *Chem. Rev.*, **108** (8), 2952–3015.

16 Kade, M.J., Burke, D.J., and Hawker, C.J. (2010) The power of thiol-ene chemistry. *J. Polym. Sci., Part A: Polym. Chem.*, **48** (4), 743–750.

17 Altintas, O., Vogt, A.P., Barner-Kowollik, C., and Tunca, U. (2012) Constructing star polymersvia modular ligation strategies. *Polym. Chem.*, **3** (1), 34–45.

18 Pomposo, J.A. (2014) Bioinspired single-chain polymer nanoparticles. *Polym. Int.*, **63** (4), 589–592.

19 Pomposo, J.A., Perez-Baena, I., Lo Verso, F., Moreno, A.J., Arbe, A., and Colmenero, J. (2014) How Far Are single-chain polymer nanoparticles in solution from the globular state? *ACS Macro Lett.*, **3** (8), 767–772.

20 Sanchez-Sanchez, A. and Pomposo, J.A. (2014) Single-chain polymer nanoparticles via non-covalent and dynamic covalent bonds. *Part. Part. Syst. Charact.*, **31** (1), 11–23.

21 Terashima, T. (2014) Functional spaces in star and single-chain polymers via living radical polymerization. *Polym. J.*, **46** (10), 664–673.

22 Frank, P., Prasher, A., Tuten, B., Chao, D., and Berda, E. (2015) Characterization of single-chain polymer folding using size exclusion chromatography with multiple modes of detection. *Appl. Petrochem. Res.*, **5** (1), 9–17.

23 Gonzalez-Burgos, M., Latorre-Sanchez, A., and Pomposo, J.A. (2015) Advances in single chain technology. *Chem. Soc. Rev.*, **44** (17), 6122–6142.

24 Lyon, C.K., Prasher, A., Hanlon, A.M., Tuten, B.T., Tooley, C.A., Frank, P.G., and Berda, E.B. (2015) A brief user's guide to single-chain nanoparticles. *Polym. Chem.*, **6** (2), 181–197.

25 Mavila, S., Eivgi, O., Berkovich, I., and Lemcoff, N.G. (2016) Intramolecular cross-linking methodologies for the synthesis of polymer nanoparticles. *Chem. Rev.*, **116** (3), 878–961.

26 Altintas, O. and Barner-Kowollik, C. (2016) Single-chain folding of synthetic polymers: a critical update. *Macromol. Rapid Commun.*, **37** (1), 29–46.

27 Hanlon, A.M., Lyon, C.K., and Berda, E.B. (2016) What is next in single-chain nanoparticles? *Macromolecules*, **49** (1), 2–14.

28 Lehn, J.-M. (1990) Perspectives in supramolecular chemistry - from molecular recognition towards molecular information processing and self-organization. *Angew. Chem. Int. Ed.*, **29**, 1304–1319.

29 Dill, K.A. and MacCallum, J.L. (2012) The protein-folding problem, 50 years on. *Science*, **338**, 1042–1046.

30 Artar, M., Huerta, E., Meijer, E.W., and Palmans, A.R.A. (2014) Dynamic single chain polymeric nanoparticles: from structure to function, in *Sequence-controlled polymers: synthesis, self-assembly, and properties*, vol. **1170** (eds J.-F. Lutz, T.Y. Meyer, M. Ouchi, and M. Sawamoto), American Chemical Society, Washington, DC, pp. 313–325.

31 Laurent, B.A. and Grayson, S.M. (2009) Synthetic approaches for the preparation of cyclic polymers. *Chem. Soc. Rev.*, **38** (8), 2202–2213.

32 Josse, T., De Winter, J., Gerbaux, P., and Coulembier, O. (2016) Cyclic polymers by ring-closure strategies. *Angew. Chem. Int. Ed.*, **55** (45), 13944–13958.

33 Kricheldorf, H.R. (2009) Simultaneous chain-growth and step-growth polymerization—a New route to cyclic polymers. *Macromol. Rapid Commun.*, **30** (16), 1371–1381.

34 Laurent, B.A. and Grayson, S.M. (2006) An efficient route to well-defined macrocyclic polymers via "click" cyclization. *J. Am. Chem. Soc.*, **128** (13), 4238–4239.

35 Eugene, D.M. and Grayson, S.M. (2008) Efficient preparation of cyclic poly(methyl acrylate)-block-poly(styrene) by combination of atom transfer radical polymerization and click cyclization. *Macromolecules*, **41** (14), 5082–5084.

36 Goldmann, A.S., Quémener, D., Millard, P.-E., Davis, T.P., Stenzel, M.H., Barner-Kowollik, C., and Müller, A.H.E. (2008) Access to cyclic polystyrenes via a combination of reversible addition fragmentation chain transfer (RAFT) polymerization and click chemistry. *Polymer*, **49** (9), 2274–2281.

37 Schmidt, B.V.K.J., Fechler, N., Falkenhagen, J., and Lutz, J.-F. (2011) Controlled folding of synthetic polymer chains through the formation of positionable covalent bridges. *Nat. Chem.*, **3** (3), 234–238.

38 Sugai, N., Heguri, H., Yamamoto, T., and Tezuka, Y. (2011) A programmed polymer folding: click and clip construction of doubly fused tricyclic and triply fused tetracyclic polymer topologies. *J. Am. Chem. Soc.*, **133** (49), 19694–19697.

39 Josse, T., Altintas, O., Oehlenschlaeger, K.K., Dubois, P., Gerbaux, P., Coulembier, O., and Barner-Kowollik, C. (2014) Ambient temperature catalyst-free light-induced preparation of macrocyclic aliphatic polyesters. *Chem. Commun.*, **50** (16), 2024–2026.

40 Josse, T., De Winter, J., Altintas, O., Dubois, P., Barner-Kowollik, C., Gerbaux, P., and Coulembier, O. (2015) A sunlight-induced click reaction as an efficient route to cyclic aliphatic polyesters. *Macromol. Chem. Phys.*, **216** (11), 1227–1234.

41 Tang, Q., Wu, Y., Sun, P., Chen, Y., and Zhang, K. (2014) Powerful ring-closure method for preparing varied cyclic polymers. *Macromolecules*, **47** (12), 3775–3781.

42 Oehlenschlaeger, K.K., Mueller, J.O., Heine, N.B., Glassner, M., Guimard, N.K., Delaittre, G., Schmidt, F.G., and Barner-Kowollik, C. (2013)

Light-induced modular ligation of conventional RAFT polymers. *Angew. Chem. Int. Ed.*, **52** (2), 762–766.

43 Sun, P., Liu, J., Zhang, Z., and Zhang, K. (2016) Scalable preparation of cyclic polymers by the ring-closure method assisted by the continuous-flow technique. *Polym. Chem.*, **7** (12), 2239–2244.

44 Yamamoto, T., Yagyu, S., and Tezuka, Y. (2016) Light- and heat-triggered reversible linear–cyclic topological conversion of telechelic polymers with anthryl End groups. *J. Am. Chem. Soc.*, **138** (11), 3904–3911.

45 Lu, D., Jia, Z., and Monteiro, M.J. (2013) Synthesis of alkyne functional cyclic polymers by one-pot thiol-ene cyclization. *Polym. Chem.*, **4** (6), 2080–2089.

46 Hoyle, C.E. and Bowman, C.N. (2010) Thiol–Ene click chemistry. *Angew. Chem. Int. Ed.*, **49** (9), 1540–1573.

47 Zhao, J., Zhou, Y., Zhou, Y., Zhou, N., Pan, X., Zhang, Z., and Zhu, X. (2016) A straightforward approach for the one-pot synthesis of cyclic polymers from RAFT polymers via thiol-michael addition. *Polym. Chem.*, **7** (9), 1782–1791.

48 Stamenović, M.M., Espeel, P., Baba, E., Yamamoto, T., Tezuka, Y., and Du Prez, F.E. (2013) Straightforward synthesis of functionalized cyclic polymers in high yield via RAFT and thiolactone-disulfide chemistry. *Polym. Chem.*, **4** (1), 184–193.

49 Altintas, O., Gerstel, P., Dingenouts, N., and Barner-Kowollik, C. (2010) Single chain self-assembly: preparation of [small alpha],[small omega]-donor-acceptor chains via living radical polymerization and orthogonal conjugation. *Chem. Commun.*, **46** (34), 6291–6293.

50 Altintas, O., Rudolph, T., and Barner-Kowollik, C. (2011) Single chain self-assembly of well-defined heterotelechelic polymers generated by ATRP and click chemistry revisited. *J. Polym. Sci., Part A: Polym. Chem.*, **49** (12), 2566–2576.

51 Altintas, O., Lejeune, E., Gerstel, P., and Barner-Kowollik, C. (2012) Bioinspired dual self-folding of single polymer chains via reversible hydrogen bonding. *Polym. Chem.*, **3** (3), 640–651.

52 Altintas, O., Krolla-Sidenstein, P., Gliemann, H., and Barner-Kowollik, C. (2014) Single-chain folding of diblock copolymers driven by orthogonal H-donor and acceptor units. *Macromolecules*, **47** (17), 5877–5888.

53 Inoue, Y., Kuad, P., Okumura, Y., Takashima, Y., Yamaguchi, H., and Harada, A. (2007) Thermal and photochemical switching of conformation of poly(ethylene glycol)-substituted cyclodextrin with an azobenzene group at the chain End. *J. Am. Chem. Soc.*, **129** (20), 6396–6397.

54 Willenbacher, J., Schmidt, B.V.K.J., Schulze-Suenninghausen, D., Altintas, O., Luy, B., Delaittre, G., and Barner-Kowollik, C. (2014) Reversible single-chain selective point folding via cyclodextrin driven host-guest chemistry in water. *Chem. Commun.*, **50** (53), 7056–7059.

55 Willenbacher, J., Altintas, O., Roesky, P.W., and Barner-Kowollik, C. (2014) Single-chain self-folding of synthetic polymers induced by metal–ligand complexation. *Macromol. Rapid Commun.*, **35** (1), 45–51.

56 Longi, P., Greco, F., and Rossi, U. (1969) Polymers containing intramolecular crosslinks. *Makromol. Chem.*, **129** (1), 157–164.

57 Harth, E., Horn, B.V., Lee, V.Y., Germack, D.S., Gonzales, C.P., Miller, R.D., and Hawker, C.J. (2002) A facile approach to architecturally defined nanoparticles via intramolecular chain collapse. *J. Am. Chem. Soc.*, **124** (29), 8653–8660.

58 Pyun, J., Tang, C., Kowalewski, T., Fréchet, J.M.J., and Hawker, C.J. (2005) Synthesis and direct visualization of block copolymers composed of different macromolecular architectures. *Macromolecules*, **38** (7), 2674–2685.

59 Tuteja, A., Mackay, M.E., Hawker, C.J., Van Horn, B., and Ho, D.L. (2006) Molecular architecture and rheological characterization of novel intramolecularly crosslinked polystyrene nanoparticles. *J. Polym. Sci., Part B: Polym. Phys.*, **44** (14), 1930–1947.

60 Croce, T.A., Hamilton, S.K., Chen, M.L., Muchalski, H., and Harth, E. (2007) Alternative o-quinodimethane cross-linking precursors for intramolecular chain collapse nanoparticles. *Macromolecules*, **40** (17), 6028–6031.

61 Adkins, C.T., Muchalski, H., and Harth, E. (2009) Nanoparticles with individual site-isolated semiconducting polymers from intramolecular chain collapse processes. *Macromolecules*, **42** (15), 5786–5792.

62 Dobish, J.N., Hamilton, S.K., and Harth, E. (2012) Synthesis of low-temperature benzocyclobutene cross-linker and utilization. *Polym. Chem.*, **3** (4), 857–860.

63 Oria, L., Aguado, R., Pomposo, J.A., and Colmenero, J. (2010) A versatile "click" chemistry precursor of functional polystyrene nanoparticles. *Adv. Mater.*, **22** (28), 3038–3041.

64 Ormategui, N., Garcia, I., Padro, D., Cabanero, G., Grande, H.J., and Loinaz, I. (2012) Synthesis of single chain thermoresponsive polymer nanoparticles. *Soft Matter*, **8** (3), 734–740.

65 de Luzuriaga, A.R., Perez-Baena, I., Montes, S., Loinaz, I., Odriozola, I., García, I., and Pomposo, J.A. (2010) New route to polymeric nanoparticles by click chemistry using bifunctional cross-linkers. *Macromol. Symp.*, **296** (1), 303–310.

66 de Luzuriaga, A.R., Ormategui, N., Grande, H.J., Odriozola, I., Pomposo, J.A., and Loinaz, I. (2008) Intramolecular click cycloaddition: an efficient room-temperature route towards bioconjugable polymeric nanoparticles. *Macromol. Rapid Commun.*, **29** (12–13), 1156–1160.

67 Sanchez-Sanchez, A., Asenjo-Sanz, I., Buruaga, L., and Pomposo, J.A. (2012) Naked and self-clickable propargylic-decorated single-chain nanoparticle precursors via redox-initiated RAFT polymerization. *Macromol. Rapid Commun.*, **33** (15), 1262–1267.

68 Hoyle, C.E., Lowe, A.B., and Bowman, C.N. (2010) Thiol-click chemistry: a multifaceted toolbox for small molecule and polymer synthesis. *Chem. Soc. Rev.*, **39** (4), 1355–1387.

69 Perez-Baena, I., Asenjo-Sanz, I., Arbe, A., Moreno, A.J., Lo Verso, F., Colmenero, J., and Pomposo, J.A. (2014) Efficient route to compact

single-chain nanoparticles: photoactivated synthesis via thiol–Yne coupling reaction. *Macromolecules*, **47** (23), 8270–8280.

70 Altintas, O., Willenbacher, J., Wuest, K.N.R., Oehlenschlaeger, K.K., Krolla-Sidenstein, P., Gliemann, H., and Barner-Kowollik, C. (2013) A mild and efficient approach to functional single-chain polymeric nanoparticles via photoinduced diels–alder ligation. *Macromolecules*, **46** (20), 8092–8101.

71 Zhu, B., Qian, G., Xiao, Y., Deng, S., Wang, M., and Hu, A. (2011) A convergence of photo-Bergman cyclization and intramolecular chain collapse towards polymeric nanoparticles. *J. Polym. Sci., Part A: Polym. Chem.*, **49** (24), 5330–5338.

72 Willenbacher, J., Wuest, K.N.R., Mueller, J.O., Kaupp, M., Wagenknecht, H.-A., and Barner-Kowollik, C. (2014) Photochemical design of functional fluorescent single-chain nanoparticles. *ACS Macro Lett.*, **3** (6), 574–579.

73 Hansell, C.F., Lu, A., Patterson, J.P., and O'Reilly, R.K. (2014) Exploiting the tetrazine-norbornene reaction for single polymer chain collapse. *Nanoscale*, **6** (8), 4102–4107.

74 Li, G., Tao, F., Wang, L., Li, Y., and Bai, R. (2014) A facile strategy for preparation of single-chain polymeric nanoparticles by intramolecular photo-crosslinking of azide polymers. *Polymer*, **55** (16), 3696–3702.

75 Frank, P.G., Tuten, B.T., Prasher, A., Chao, D., and Berda, E.B. (2014) Intra-chain photodimerization of pendant anthracene units as an efficient route to single-chain nanoparticle fabrication. *Macromol. Rapid Commun.*, **35** (2), 249–253.

76 Fan, W., Tong, X., Yan, Q., Fu, S., and Zhao, Y. (2014) Photodegradable and size-tunable single-chain nanoparticles prepared from a single main-chain coumarin-containing polymer precursor. *Chem. Commun.*, **50** (88), 13492–13494.

77 He, J., Tremblay, L., Lacelle, S., and Zhao, Y. (2011) Preparation of polymer single chain nanoparticles using intramolecular photodimerization of coumarin. *Soft Matter*, **7** (6), 2380–2386.

78 Njikang, G., Liu, G., and Curda, S.A. (2008) Tadpoles from the intramolecular photo-cross-linking of diblock copolymers. *Macromolecules*, **41** (15), 5697–5702.

79 Zhou, F., Xie, M., and Chen, D. (2014) Structure and ultrasonic sensitivity of the superparticles formed by self-assembly of single chain janus nanoparticles. *Macromolecules*, **47** (1), 365–372.

80 Mecerreyes, D., Lee, V., Hawker, C.J., Hedrick, J.L., Wursch, A., Volksen, W., Magbitang, T., Huang, E., and Miller, R.D. (2001) A novel approach to functionalized nanoparticles: self-crosslinking of macromolecules in ultradilute solution. *Adv. Mater.*, **13** (3), 204–208.

81 Jiang, J. and Thayumanavan, S. (2005) Synthesis and characterization of amine-functionalized polystyrene nanoparticles. *Macromolecules*, **38** (14), 5886–5891.

82 Dirlam, P.T., Kim, H.J., Arrington, K.J., Chung, W.J., Sahoo, R., Hill, L.J., Costanzo, P.J., Theato, P., Char, K., and Pyun, J. (2013) Single chain polymer nanoparticles via sequential ATRP and oxidative polymerization. *Polym. Chem.*, **4** (13), 3765–3773.

83 Watanabe, K., Tanaka, R., Takada, K., Kim, M.-J., Lee, J.-S., Tajima, K., Isono, T., and Satoh, T. (2016) Intramolecular olefin metathesis as a robust tool to synthesize single-chain nanoparticles in a size-controlled manner. *Polym. Chem.*, **7** (29), 4782–4792.

84 Bai, Y., Xing, H., Vincil, G.A., Lee, J., Henderson, E.J., Lu, Y., Lemcoff, N.G., and Zimmerman, S.C. (2014) Practical synthesis of water-soluble organic nanoparticles with a single reactive group and a functional carrier scaffold. *Chem. Sci.*, **5** (7), 2862–2868.

85 Li, W., Kuo, C.-H., Kanyo, I., Thanneeru, S., and He, J. (2014) Synthesis and self-assembly of amphiphilic hybrid nano building blocks via self-collapse of polymer single chains. *Macromolecules*, **47** (17), 5932–5941.

86 Taranekar, P., Park, J.Y., Patton, D., Fulghum, T., Ramon, G.J., and Advincula, R. (2006) Conjugated polymer nanoparticles via intramolecular crosslinking of dendrimeric precursors. *Adv. Mater.*, **18** (18), 2461–2465.

87 Wong, E.H.H. and Qiao, G.G. (2015) Factors influencing the formation of single-chain polymeric nanoparticles prepared via ring-opening polymerization. *Macromolecules*, **48** (5), 1371–1379.

88 Perez-Baena, I., Barroso-Bujans, F., Gasser, U., Arbe, A., Moreno, A.J., Colmenero, J., and Pomposo, J.A. (2013) Endowing single-chain polymer nanoparticles with enzyme-mimetic activity. *ACS Macro Lett.*, **2** (9), 775–779.

89 Cherian, A.E., Sun, F.C., Sheiko, S.S., and Coates, G.W. (2007) Formation of nanoparticles by intramolecular cross-linking: following the reaction progress of single polymer chains by atomic force microscopy. *J. Am. Chem. Soc.*, **129** (37), 11350–11351.

90 Wong, E.H.H., Lam, S.J., Nam, E., and Qiao, G.G. (2014) Biocompatible single-chain polymeric nanoparticles via organo-catalyzed ring-opening polymerization. *ACS Macro Lett.*, **3** (6), 524–528.

91 Beck, J.B., Killops, K.L., Kang, T., Sivanandan, K., Bayles, A., Mackay, M.E., Wooley, K.L., and Hawker, C.J. (2009) Facile preparation of nanoparticles by intramolecular cross-linking of isocyanate functionalized copolymers. *Macromolecules*, **42** (15), 5629–5635.

92 Zhang, Y. and Zhao, H. (2015) Surface-tunable colloidal particles stabilized by mono-tethered single-chain nanoparticles. *Polymer*, **64**, 277–284.

93 Sanchez-Sanchez, A. and Pomposo, J. (2015) Efficient synthesis of single-chain polymer nanoparticles via amide formation. *J. Nanomater.*, **2015**, 7.

94 Roy, R.K. and Lutz, J.-F. (2014) Compartmentalization of single polymer chains by stepwise intramolecular cross-linking of sequence-controlled macromolecules. *J. Am. Chem. Soc.*, **136** (37), 12888–12891.

95 Wang, P., Pu, H., Ge, J., Jin, M., Pan, H., Chang, Z., and Wan, D. (2014) Fluorescence-labeled hydrophilic nanoparticles via single-chain folding. *Mater. Lett.*, **132**, 102–105.

96 Jiang, X., Pu, H., and Wang, P. (2011) Polymer nanoparticles via intramolecular crosslinking of sulfonyl azide functionalized polymers. *Polymer*, **52** (16), 3597–3602.

97 Wang, P., Pu, H., and Jin, M. (2011) Single-chain nanoparticles with well-defined structure via intramolecular crosslinking of linear polymers with pendant benzoxazine groups. *J. Polym. Sci., Part A: Polym Chem.*, **49** (24), 5133–5141.

98 Zheng, H., Ye, X., Wang, H., Yan, L., Bai, R., and Hu, W. (2011) A facile one-pot strategy for preparation of small polymer nanoparticles by self-crosslinking of amphiphilic block copolymers containing acyl azide groups in aqueous media. *Soft Matter*, **7** (8), 3956–3962.

99 Wen, J., Zhang, J., Zhang, Y., Yang, Y., and Zhao, H. (2014) Controlled self-assembly of amphiphilic monotailed single-chain nanoparticles. *Polym. Chem.*, **5** (13), 4032–4038.

100 Radu, J.É.F., Novak, L., Hartmann, J.F., Beheshti, N., Kjøniksen, A.-L., Nyström, B., and Borbély, J. (2008) Structural and dynamical characterization of poly-gamma-glutamic acid-based cross-linked nanoparticles. *Colloid Polym. Sci.*, **286** (4), 365–376.

101 Chao, D., Jia, X., Tuten, B., Wang, C., and Berda, E.B. (2013) Controlled folding of a novel electroactive polyolefin via multiple sequential orthogonal intra-chain interactions. *Chem. Commun.*, **49** (39), 4178–4180.

102 Cheng, R.P., Gellman, S.H., and Degrado, W.F. (2001) Beta-peptides: from structure to function. *Chem. Rev.*, **101**, 3219–3232.

103 Mes, T., Smulders, M.M.J., Palmans, A.R.A., and Meijer, E.W. (2010) Hydrogen-bond engineering in supramolecular polymers: polarity influence on the self-assembly of benzene-1,3,5-tricarboxamides. *Macromolecules*, **43** (4), 1981–1991.

104 Mes, T., van der Weegen, R., Palmans, A.R., and Meijer, E.W. (2011) Single-chain polymeric nanoparticles by stepwise folding. *Angew. Chem. Int. Ed.*, **50** (22), 5085–5089.

105 Stals, P.J.M., Gillissen, M.A.J., Paffen, T.F.E., de Greef, T.F.A., Lindner, P., Meijer, E.W., Palmans, A.R.A., and Voets, I.K. (2014) Folding polymers with pendant hydrogen bonding motifs in water: the effect of polymer length and concentration on the shape and size of single-chain polymeric nanoparticles. *Macromolecules*, **47** (9), 2947–2954.

106 Stals, P.J.M., Cheng, C.-Y., van Beek, L., Wauters, A.C., Palmans, A.R.A., Han, S., and Meijer, E.W. (2016) Surface water retardation around single-chain polymeric nanoparticles: critical for catalytic function? *Chem. Sci.*, **7** (3), 2011–2015.

107 Huerta, E., Stals, P.J., Meijer, E.W., and Palmans, A.R. (2013) Consequences of folding a water-soluble polymer around an organocatalyst. *Angew. Chem. Int. Ed.*, **52** (10), 2906–2910.

108 Artar, M., Terashima, T., Sawamoto, M., Meijer, E.W., and Palmans, A.R.A. (2014) Understanding the catalytic activity of single-chain polymeric nanoparticles in water. *J. Polym. Sci., Part A: Polym. Chem.*, **52** (1), 12–20.

109 Huerta, E., van Genabeek, B., Stals, P.J., Meijer, E.W., and Palmans, A.R. (2014) A modular approach to introduce function into single-chain polymeric nanoparticles. *Macromol. Rapid Commun.*, **35** (15), 1320–1325.

110 Hosono, N., Kushner, A.M., Chung, J., Palmans, A.R., Guan, Z., and Meijer, E.W. (2015) Forced unfolding of single-chain polymeric nanoparticles. *J. Am. Chem. Soc.*, **137** (21), 6880–6888.

111 Foster, E.J., Berda, E.B., and Meijer, E.W. (2009) Metastable supramolecular polymer nanoparticles via intramolecular collapse of single polymer chains. *J. Am. Chem. Soc.*, **131**, 6964–6966.

112 Berda, E.B., Foster, E.J., and Meijer, E.W. (2010) Toward controlling folding in synthetic polymers: fabricating and characterizing supramolecular single-chain nanoparticles. *Macromolecules*, **43**, 1430–1437.

113 Foster, E.J., Berda, E.B., and Meijer, E.W. (2011) Tuning the size of supramolecular single-chain polymer nanoparticles. *J. Polym. Sci., Part A: Polym. Chem.*, **49** (1), 118–126.

114 Stals, P.J.M., Gillissen, M.A.J., Nicolaÿ, R., Palmans, A.R.A., and Meijer, E.W. (2013) The balance between intramolecular hydrogen bonding, polymer solubility and rigidity in single-chain polymeric nanoparticles. *Polym. Chem.*, **4** (8), 2584.

115 van Roekel, H.W.H., Stals, P.J.M., Gillissen, M.A.J., Hilbers, P.A.J., Markvoort, A.J., and de Greef, T.F.A. (2013) Evaporative self-assembly of single-chain, polymeric nanoparticles. *Chem. Commun.*, **49**, 3122.

116 Seo, M., Beck, B.J., Paulusse, J.M.J., Hawker, C.J., and Kim, S.Y. (2008) Polymeric nanoparticles via noncovalent cross-linking of linear chains. *Macromolecules*, **41**, 6413–6418.

117 Romulus, J. and Weck, M. (2013) Single-chain polymer self-assembly using complementary hydrogen bonding units. *Macromol. Rapid Commun.*, **34** (19), 1518–1523.

118 Hosono, N., Gillissen, M.A., Li, Y., Sheiko, S.S., Palmans, A.R., and Meijer, E.W. (2013) Orthogonal self-assembly in folding block copolymers. *J. Am. Chem. Soc.*, **135** (1), 501–510.

119 Chang, S.-K. and Hamilton, A.D. (1988) Molecular recognition of biologically interesting substrates: synthesis of an artificial receptor for barbiturates employing Six hydrogen bonds. *J. Am. Chem. Soc.*, **110**, 1318–1319.

120 Hager, K., Hartnagel, U., and Hirsch, A. (2007) Supramolecular dendrimers self-assembled from dendritic fullerene ligands and a homotritopic hamilton receptor. *Eur. J. Org. Chem.*, **2007** (12), 1942–1956.

121 Hager, K., Franz, A., and Hirsch, A. (2006) Self-assembly of chiral depsipeptide dendrimers. *Chem. Eur. J.*, **12** (10), 2663–2679.

122 Altintas, O., Artar, M., ter Huurne, G., Voets, I.K., Palmans, A.R.A., Barner-Kowollik, C., and Meijer, E.W. (2015) Design and synthesis of triblock copolymers for creating complex secondary structures by orthogonal self-assembly. *Macromolecules*, **48** (24), 8921–8932.

123 Dong, S., Luo, Y., Yan, X., Zheng, B., Ding, X., Yu, Y., Ma, Z., Zhao, Q., and Huang, F. (2011) A dual-responsive supramolecular polymer gel formed by crown ether based molecular recognition. *Angew. Chem. Int. Ed.*, **50** (8), 1905–1909.

124 Ge, Z., Hu, J., Huang, F., and Liu, S. (2009) Responsive supramolecular gels constructed by crown ether based molecular recognition. *Angew. Chem. Int. Ed.*, **48** (10), 1798–1802.

125 Zhang, M., Xu, D., Yan, X., Chen, J., Dong, S., Zheng, B., and Huang, F. (2012) Self-healing supramolecular gels formed by crown ether based host-guest interactions. *Angew. Chem. Int. Ed.*, **51** (28), 7011–7015.

126 Chen, L., Tian, Y.-K., Ding, Y., Tian, Y.-J., and Wang, F. (2012) Multistimuli responsive supramolecular cross-linked networks on the basis of the benzo-21-crown-7/secondary ammonium salt recognition motif. *Macromolecules*, **45** (20), 8412–8419.

127 Altintas, O., Yilmaz, I., Hizal, G., and Tunca, U. (2006) Synthesis of poly(methyl methacrylate)-b-polystyrene containing a crown ether unit at the junction point via combination of atom transfer radical polymerization and nitroxide mediated radical polymerization routes. *J. Polym. Sci., Part A: Polym. Chem.*, **44** (10), 3242–3249.

128 Fischer, T.S., Schulze-Sünninghausen, D., Luy, B., Altintas, O., and Barner-Kowollik, C. (2016) Stepwise unfolding of single-chain nanoparticles by chemically triggered gates. *Angew. Chem. Int. Ed.*, **55** (37), 11276–11280.

129 Yan, Q., Feng, A., Zhang, H., Yin, Y., and Yuan, J. (2013) Redox-switchable supramolecular polymers for responsive self-healing nanofibers in water. *Polym. Chem.*, **4** (4), 1216–1220.

130 Yan, Q., Yuan, J., Cai, Z., Xin, Y., Kang, Y., and Yin, Y. (2010) Voltage-responsive vesicles based on orthogonal assembly of two homopolymers. *J. Am. Chem. Soc.*, **132**, 9268–9270.

131 Lu, X. and Isaacs, L. (2016) Uptake of hydrocarbons in aqueous solution by encapsulation in acyclic cucurbit[n]uril-type molecular containers. *Angew. Chem. Int. Ed.*, **55**, 8076–8080.

132 Lagona, J., Mukhopadhyay, P., Chakrabarti, S., and Isaacs, L. (2005) The cucurbit[n]uril family. *Angew. Chem. Int. Ed.*, **44** (31), 4844–4870.

133 Appel, E.A., Dyson, J., del Barrio, J., Walsh, Z., and Scherman, O.A. (2012) Formation of single-chain polymer nanoparticles in water through host-guest interactions. *Angew. Chem. Int. Ed.*, **51** (17), 4185–4189.

134 Lu, J., Ten Brummelhuis, N., and Weck, M. (2014) Intramolecular folding of triblock copolymers via quadrupole interactions between poly(styrene) and poly(pentafluorostyrene) blocks. *Chem. Commun.*, **50**, 6225–6227.

135 Sanchez-Sanchez, A., Arbe, A., Colmenero, J., and Pomposo, J.A. (2014) Metallo-folded single-chain nanoparticles with catalytic selectivity. *ACS Macro Lett.*, **3** (5), 439–443.

136 Sanchez-Sanchez, A., Arbe, A., Kohlbrecher, J., Colmenero, J., and Pomposo, J.A. (2015) Efficient synthesis of single-chain globules mimicking the morphology and polymerase activity of metalloenzymes. *Macromol. Rapid Commun.*, **36** (17), 1592–1597.

137 Willenbacher, J., Altintas, O., Trouillet, V., Knöfel, N., Monteiro, M.J., Roesky, P.W., and Barner-Kowollik, C. (2015) Pd-complex driven formation of single-chain nanoparticles. *Polym. Chem.*, **6** (24), 4358–4365.

138 Mavila, S., Diesendruck, C.E., Linde, S., Amir, L., Shikler, R., and Lemcoff, N.G. (2013) Polycyclooctadiene complexes of rhodium(I): direct access to organometallic nanoparticles. *Angew. Chem. Int. Ed.*, **52** (22), 5767–5770.

139 Berkovich, I., Mavila, S., Iliashevsky, O., Kozuch, S., and Lemcoff, N.G. (2016) Single-chain polybutadiene organometallic nanoparticles: an experimental and theoretical study. *Chem. Sci.*, **7** (3), 1773–1778.

140 Mavila, S., Rozenberg, I., and Lemcoff, N.G. (2014) A general approach to mono- and bimetallic organometallic nanoparticles. *Chem. Sci.*, **5** (11), 4196–4203.

141 Bogdanović, B., Kröner, M., Wilke, G., and Übergangsmetallkomplexe, I. (1966) Olefin-komplexe des nickels(0). *Justus Liebigs Annalen der Chemie*, **699**, 1–23.

142 Wang, F., Pu, H., Jin, M., and Wan, D. (2016) Supramolecular nanoparticles via single-chain folding driven by ferrous ions. *Macromol. Rapid Commun.*, **37** (4), 330–336.

143 Jeong, J., Lee, Y.-J., Kim, B., Kim, B., Jung, K.-S., and Paik, H.-J. (2015) Colored single-chain polymeric nanoparticles via intramolecular copper phthalocyanine formation. *Polym. Chem.*, **6** (18), 3392–3397.

144 Terashima, T., Sugita, T., Fukae, K., and Sawamoto, M. (2014) Synthesis and single-chain folding of amphiphilic random copolymers in water. *Macromolecules*, **47**, 589–600.

145 Koda, Y., Terashima, T., and Sawamoto, M. (2016) Multimode self-folding polymers via reversible and thermoresponsive self-assembly of amphiphilic/fluorous random copolymers. *Macromolecules*, **49**, 4534–4543.

146 Hirai, Y., Terashima, T., Takenaka, M., and Sawamoto, M. (2016) Precision self-assembly of amphiphilic random copolymers into uniform and self-sorting nanocompartments in water. *Macromolecules*, **49** (14), 5084–5091.

147 Rowan, S.J., Cantrill, S.J., Cousins, G.R.L., Sanders, J.K.M., and Stoddart, J.F. (2002) Dynamic covalent chemistry. *Angew. Chem. Int. Ed.*, **41** (6), 898–952.

148 Maeda, T., Otsuka, H., and Takahara, A. (2009) Dynamic covalent polymers: reorganizable polymers with dynamic covalent bonds. *Prog. Polym. Sci.*, **34** (7), 581–604.

149 Lascano, S., Zhang, K.-D., Wehlauch, R., Gademann, K., Sakai, N., and Matile, S. (2016) The third orthogonal dynamic covalent bond. *Chem. Sci.*, **7** (7), 4720–4724.

150 Shishkan, O., Zamfir, M., Gauthier, M.A., Borner, H.G., and Lutz, J.-F. (2014) Complex single-chain polymer topologies locked by positionable twin disulfide cyclic bridges. *Chem. Commun.*, **50** (13), 1570–1572.

151 Braslau, R., Rivera Iii, F., and Tansakul, C. (2013) Reversible crosslinking of polymers bearing pendant or terminal thiol groups prepared by nitroxide-mediated radical polymerization. *React. Funct. Polym.*, **73** (4), 624–633.

152 Whitaker, D.E., Mahon, C.S., and Fulton, D.A. (2013) Thermoresponsive dynamic covalent single-chain polymer nanoparticles reversibly transform into a hydrogel. *Angew. Chem. Int. Ed.*, **52** (3), 956–959.

153 Sanchez-Sanchez, A., Fulton, D.A., and Pomposo, J.A. (2014) pH-responsive single-chain polymer nanoparticles utilising dynamic covalent enamine bonds. *Chem. Commun.*, **50** (15), 1871–1874.

154 Jin, Y., Yu, C., Denman, R.J., and Zhang, W. (2013) Recent advances in dynamic covalent chemistry. *Chem. Soc. Rev.*, **42** (16), 6634–6654.
155 Ying, H., Zhang, Y., and Cheng, J. (2014) Dynamic urea bond for the design of reversible and self-healing polymers. *Nat. Commun.*, **5**, 3218–3237.
156 Murray, B.S. and Fulton, D.A. (2011) Dynamic covalent single-chain polymer nanoparticles. *Macromolecules*, **44** (18), 7242–7252.
157 Song, C., Li, L., Dai, L., and Thayumanavan, S. (2015) Responsive single-chain polymer nanoparticles with host-guest features. *Polym. Chem.*, **6** (26), 4828–4834.
158 Buruaga, L. and Pomposo, J.A. (2011) Metal-free polymethyl methacrylate (PMMA) nanoparticles by enamine "click" chemistry at room temperature. *Polymers*, **3** (4), 1673.
159 Moreno, A.J., Lo Verso, F., Sanchez-Sanchez, A., Arbe, A., Colmenero, J., and Pomposo, J.A. (2013) Advantages of orthogonal folding of single polymer chains to soft nanoparticles. *Macromolecules*, **46** (24), 9748–9759.